

# Proton spin asymmetries and $d_2$ from SANE-HMS data

Hoyoung Kang  
For **SANE** Collaboration

Seoul National University  
APFB 2014  
April 7<sup>th</sup>, 2014



# Outline

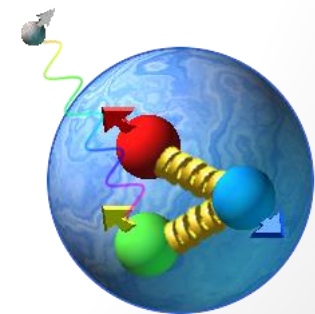
- Introduction to SANE
- Experimental Setup and SANE-HMS
- Analysis: Dilution Factor and Radiative Correction
- Result: HMS Asymmetries, Structure Functions and  $d_2$  Matrix Element
- Summary

# SANE - Spin Asymmetries on the Nucleon Experiment

Spin Asymmetries on the Nucleon Experiment, or SANE(TJNAF E07-003), is a measurement of the proton spin asymmetries

done in the Hall C of Thomas Jefferson National Accelerator Facility(Jefferson Lab), Virginia USA

during January-March 2009, excluding installation and commissioning periods.



# Spin Structure Functions

Inclusive DIS cross section depends on four structure functions, two unpolarized ( $F_1$ ,  $F_2$ ) and two polarized ( $g_1$ ,  $g_2$ ). The spin structure functions  $g_1$  and  $g_2$  can be experimentally determined by measuring spin asymmetries:

$$A_{\parallel} = \frac{\sigma^{\downarrow\uparrow} - \sigma^{\uparrow\uparrow}}{\sigma^{\downarrow\uparrow} + \sigma^{\uparrow\uparrow}}, \quad A_{\perp} = \frac{\sigma^{\downarrow\rightarrow} - \sigma^{\uparrow\rightarrow}}{\sigma^{\downarrow\rightarrow} + \sigma^{\uparrow\rightarrow}}.$$

$$g_1(x, Q^2) = \frac{F_1(x, Q^2)}{d'} [A_{\parallel} + \tan(\theta/2) A_{\perp}],$$

$$g_2(x, Q^2) = \frac{y F_1(x, Q^2)}{2d'} \left[ \frac{E + E' \cos(\theta)}{E' \sin(\theta)} A_{\perp} - A_{\parallel} \right]$$

# Spin structure functions

When the spins of electron and nucleon are all polarized, we can see the dependence of scattering cross section on the spin structure functions  $g_1(x, Q^2)$  and  $g_2(x, Q^2)$ .

$$g_1 = \frac{1}{2} \sum_i e_i^2 [q_i^+ - q_i^-]$$

$$g_2 = g_2^{WW} + \overline{g_2}$$

$$g_2^{WW}(x, Q^2) = -g_1(x, Q^2) + \int_x^1 \frac{g_1(x', Q^2)}{x'} dx'$$

# Purpose of SANE

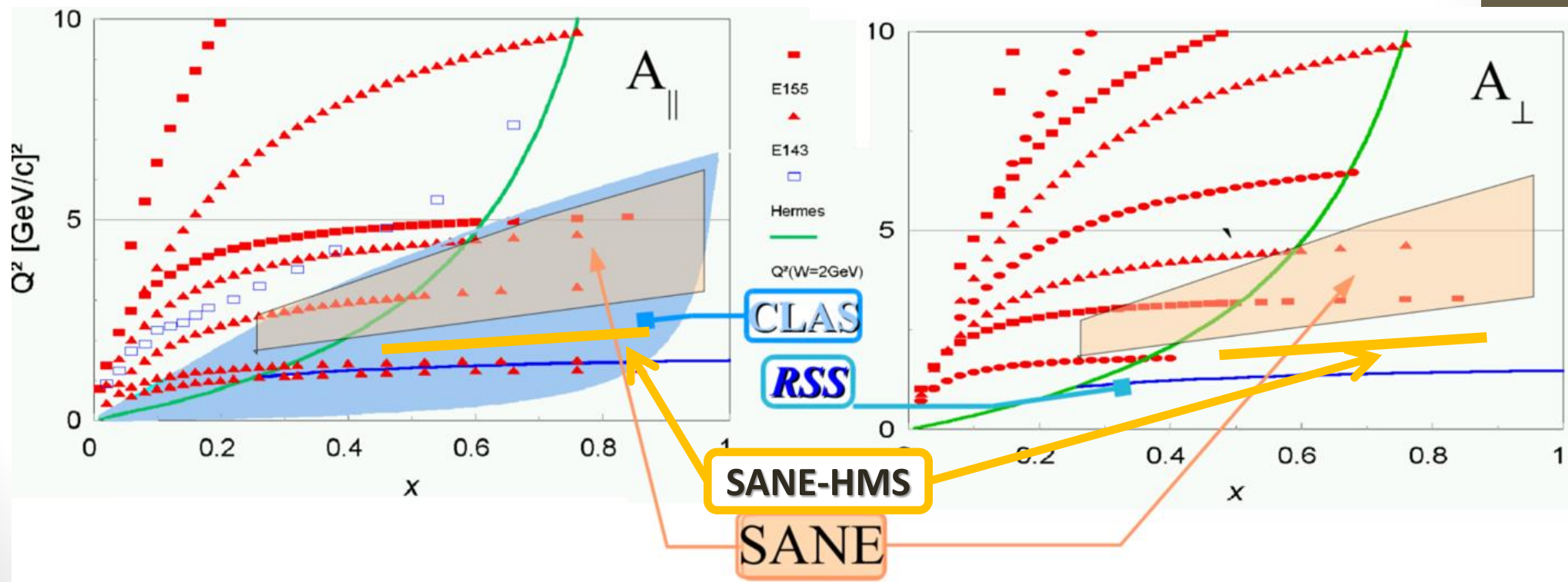
SANE's purpose is to learn everything possible about Proton Spin Asymmetries and Spin Structure Functions from Inclusive Polarized DIS:

- Resonances and  $Q^2$  dependence of  $A_2$
- SSF  $g_2(x, Q^2)$
- Twist-3 effects (higher twist represents increasing interactions among partons)
- Comparing with lattice QCD, QCD sum rules
- Exploring high Bjorken  $x$  region

# World Data and SANE Region

World data lacks big region, especially in the perpendicular asymmetry. SANE-BETA covers broad region of  $0.3 \leq x \leq 0.8$ ,  $2.5 \text{ GeV}^2 \leq Q^2 \leq 6.5 \text{ GeV}^2$

SANE-HMS covers lower  $Q^2$  region.



# Jefferson Lab CEBAF

Polarized electrons can be accelerated up to 6 *GeV* and the electron beam is continuous

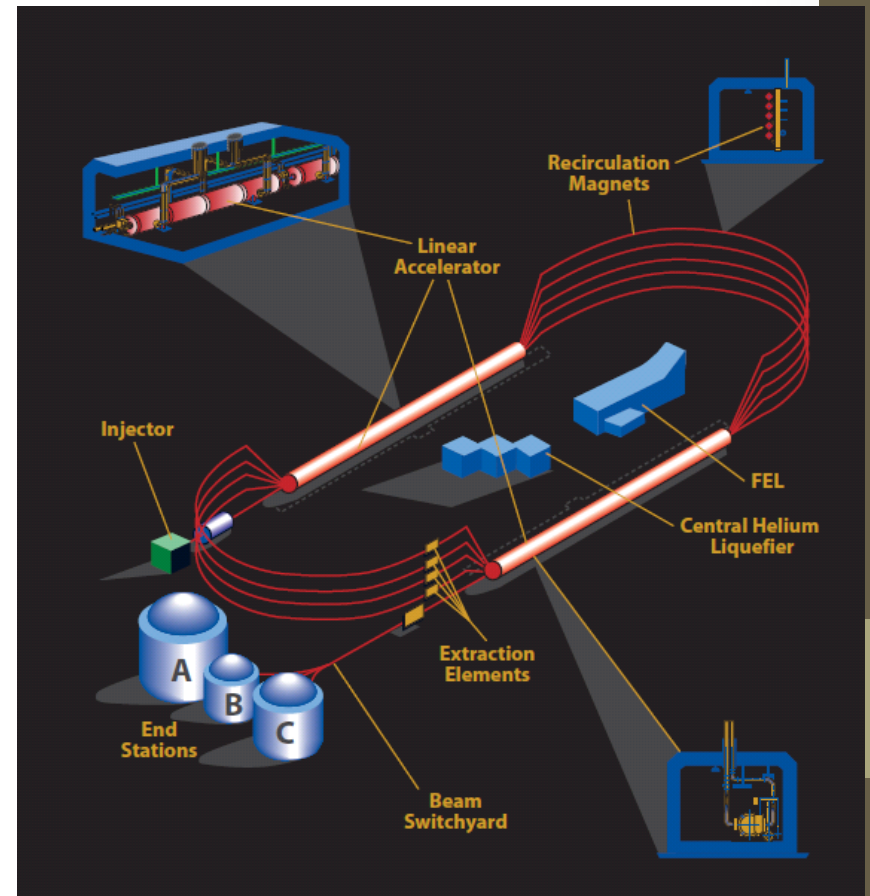
Two linear accererators and arcs

30 Hz electron helicity flip

by peudo-random basis

SANE used 4.7 and 5.9 GeV

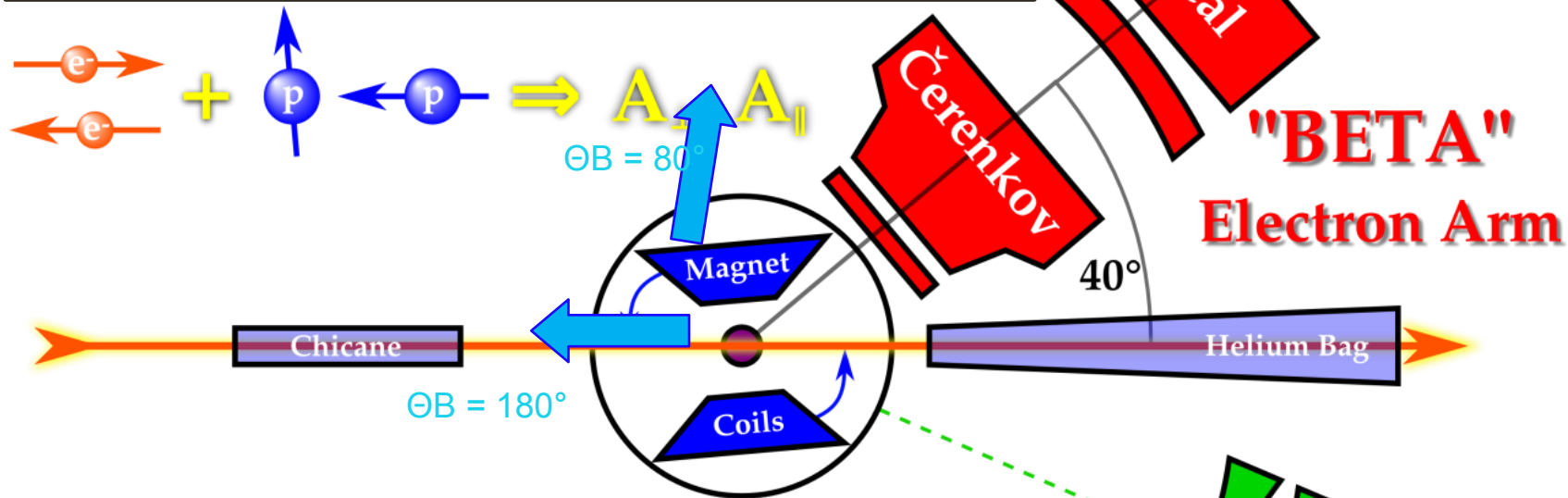
beam of 90 nA





# Experimental Setup

**Big Electron Telescope Array:**  
Broad kinematic region  
Data at intermediate  $Q^2$



**High Momentum Spectrometer:**  
Focused on small kinematic region  
Low background  
Data at lower  $Q^2$  to extend RSS results

# High Momentum Spectrometer

HMS has smaller angular acceptance than BETA, but with precise measurement.

HMS collected complementary data in SANE by varying central angle and momentum.

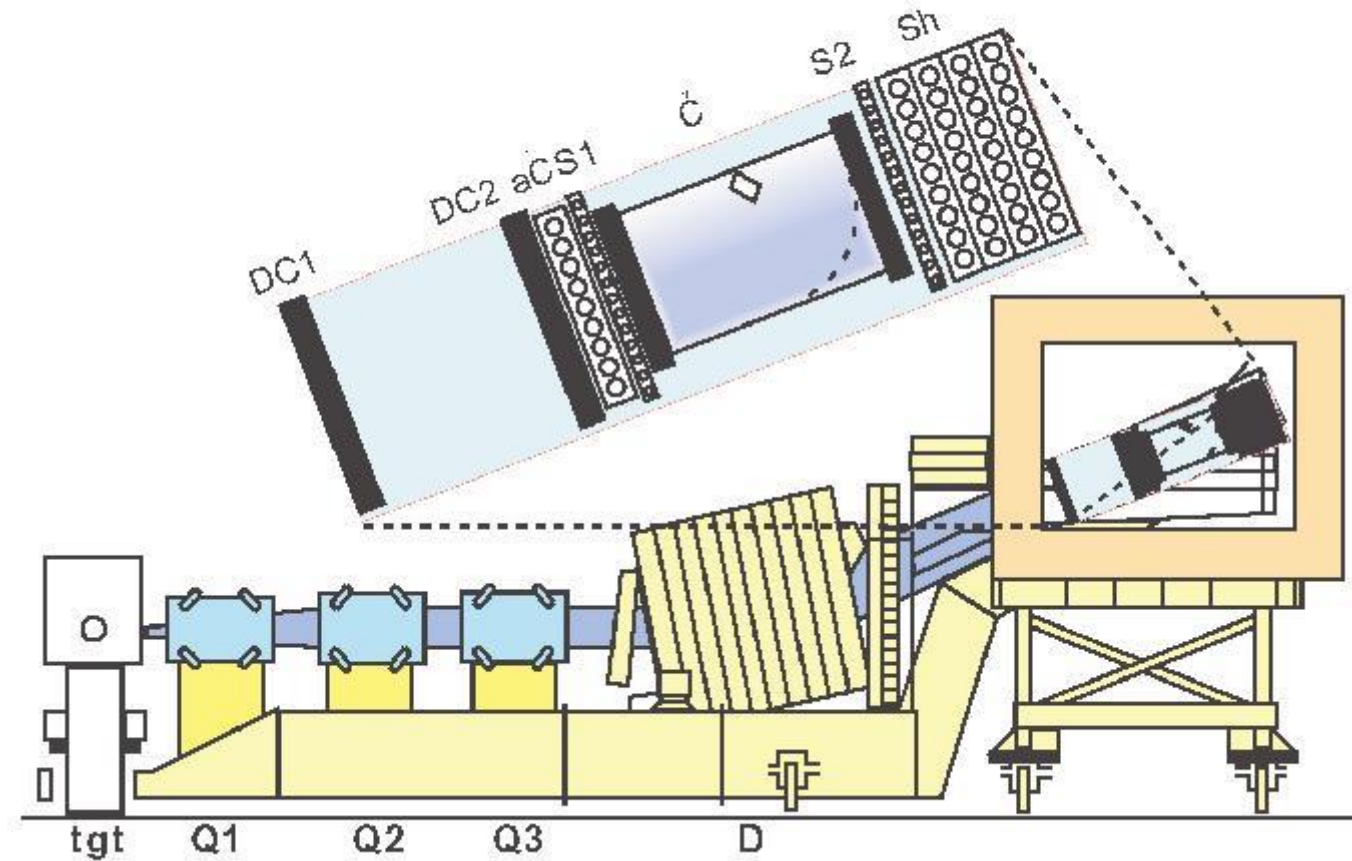
Resonance Spin Structure(RSS) experiment(2002) have produced meaningful results with limited HMS kinematics and data.

( $1.085 \text{ GeV} < W < 1.910 \text{ GeV}$  and  $\langle Q^2 \rangle = 1.3 \text{ GeV}^2$ )

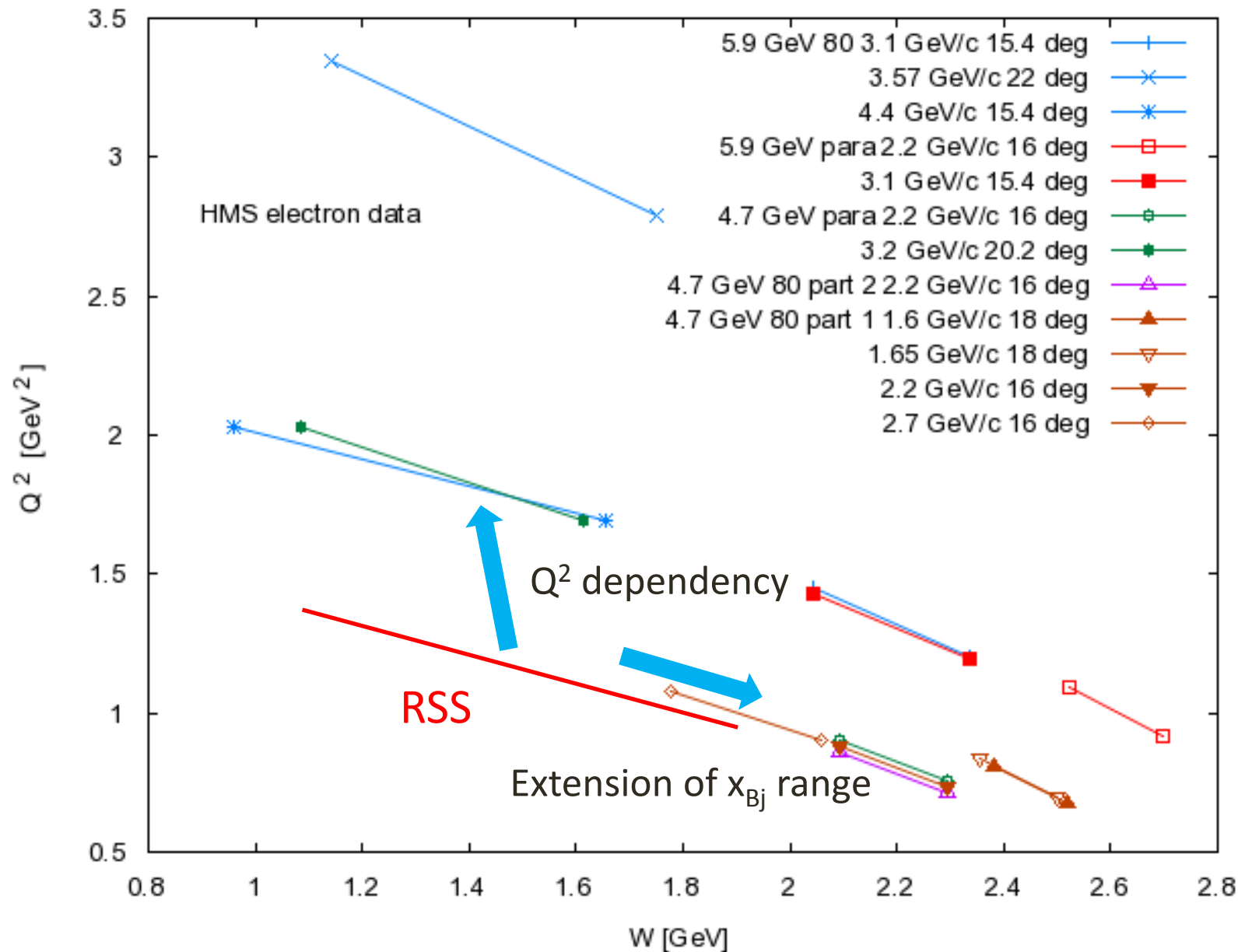
Phys. Rev. Lett. 105, 101601 (2010)

Phys. Rev. Lett. 98, 132003 (2007)

Phys. Rev. C 74, 035201 (2006)



# HMS Coverage for SANE



# Dilution Factor

## from Packing Fraction

The target and beam are not completely polarized. It contains also un-polarizable materials.

$$A = \frac{1}{P_b P_t f} \frac{d\sigma^{\downarrow\uparrow} - d\sigma^{\uparrow\uparrow}}{d\sigma^{\downarrow\uparrow} + d\sigma^{\uparrow\uparrow}}$$

Beam Polarization ~80%

Proton(target) Polarization ~70%

Dilution Factor

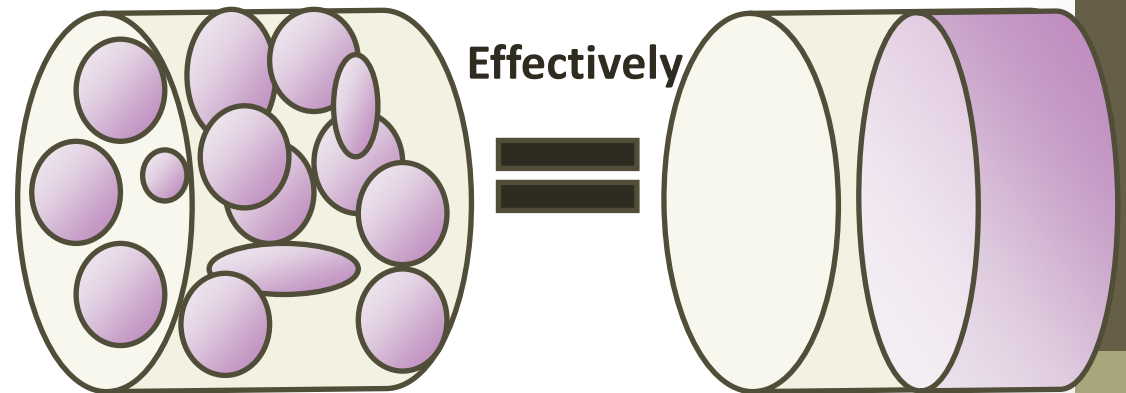
Dilution factor  $f$  is the ratio of free polarizable nucleons to the total amount of nucleons in the sample.

$$f = \frac{N_1 \sigma_1}{N_1 \sigma_1 + N_{14} \sigma_{14} + \sum N_A \sigma_A}$$

$$\text{where } N_A = \frac{N_0 \rho_A Z_A}{M_A}$$

# Dilution Factor from Packing Fraction

Packing fraction is the relative volume ratio of ammonia to the target cell, or the fraction of the cell's length that would be filled with ammonia by cylindrical symmetry.

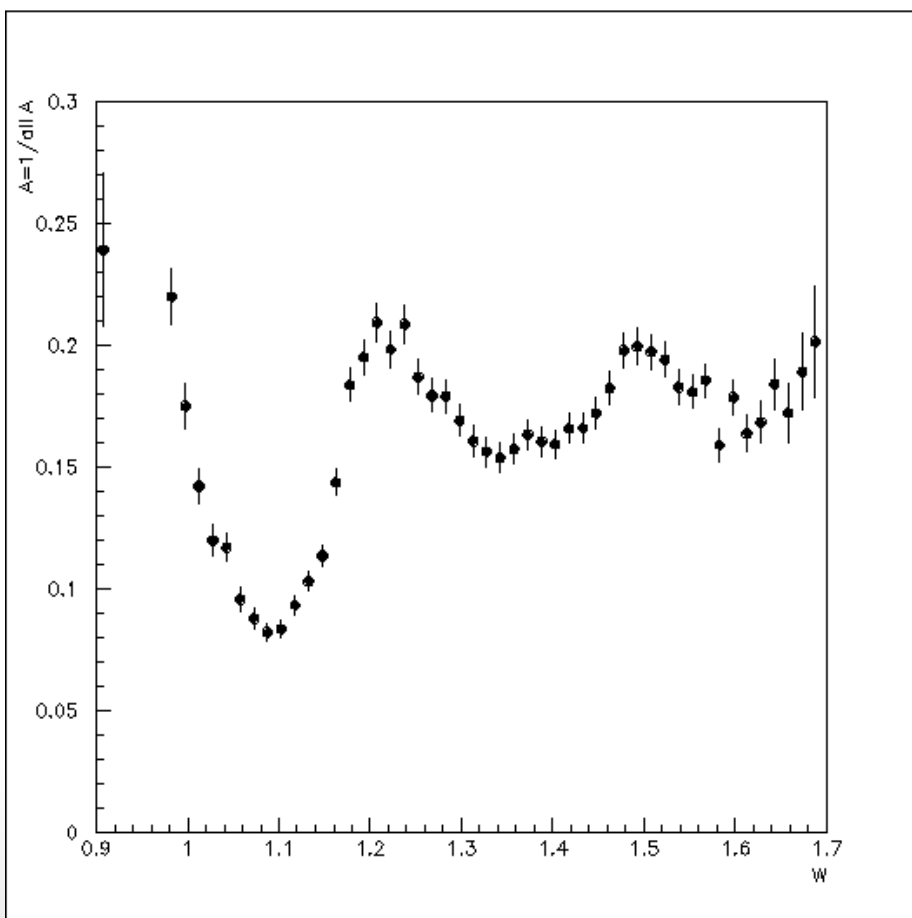


# Packing fraction

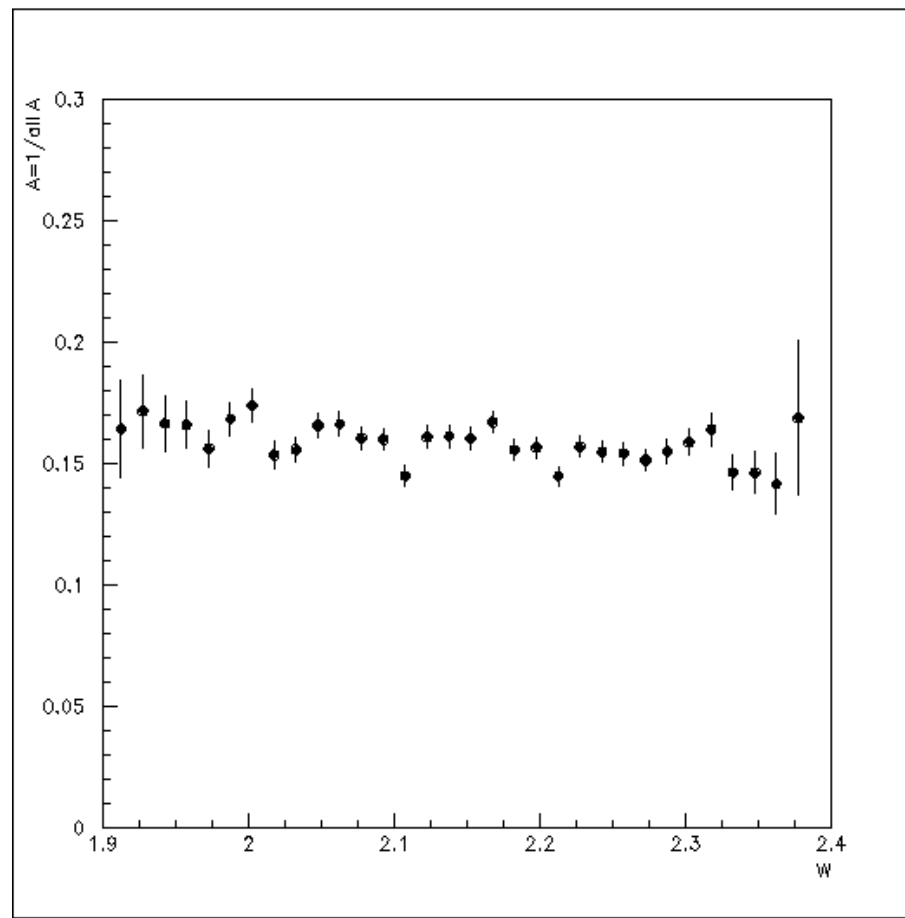
Material	PF(%)	Error(%p)
#2 JW 12/05 14NH3	61.0	4.32
14NH3 #13	60.7	4.22
#5 6-28-07 14NH3	59.6	4.47
#7 6-29-07 14NH3	59.6	4.47
#8 & 5 6-2x-07 14NH3	59.0	4.95
#5 & 6 6-2x-07 14NH3	56.9	4.74
#3 6/28/07 NIST irradi 14NH3	58.6	4.12
#2 6/28/07 NIST irradi 14NH3	58.8	4.34
#9 6-28-07 14NH3	61.9	4.59
#10 6-29-07 14NH3	59.4	4.44

# Dilution factor

Dilution factor is calculated using MC, comparing cross sections of each materials in target cell. And packing fraction is the only necessary input for each target cell.



Dilution factor of resonance region (PF 60.9%)



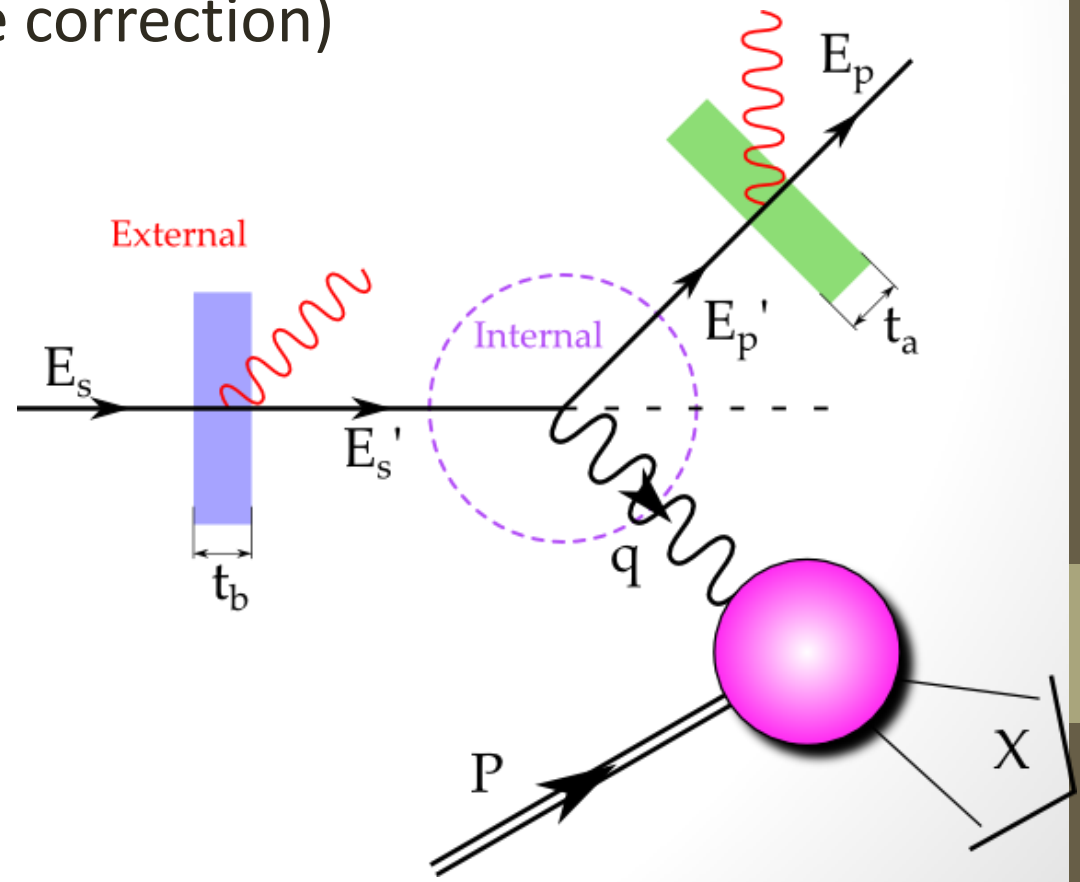
Dilution factor of DIS region (PF 57.2%)

# Radiative Correction

Following S. Stein et al., Phys. Rev. D 12, 1884 (1975),  
correction was mainly done by POLRAD 2.0

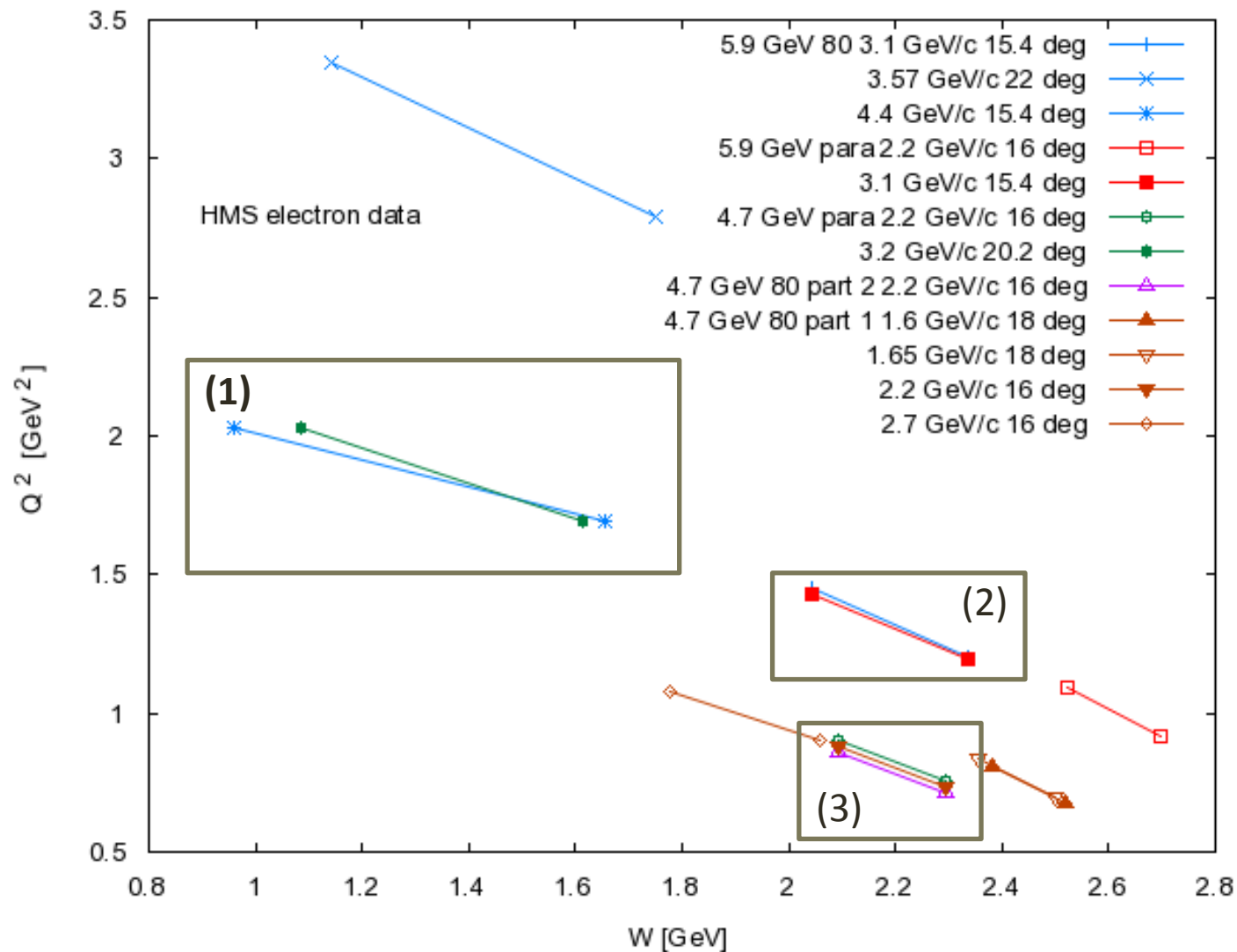
Initial fit parameters came from RSS,  
basically Breit-Wigner resonance  
and polynomial (with some correction)  
deep inelastic tail.

Newly corrected data was  
refitted to iterate.





# HMS Asymmetries



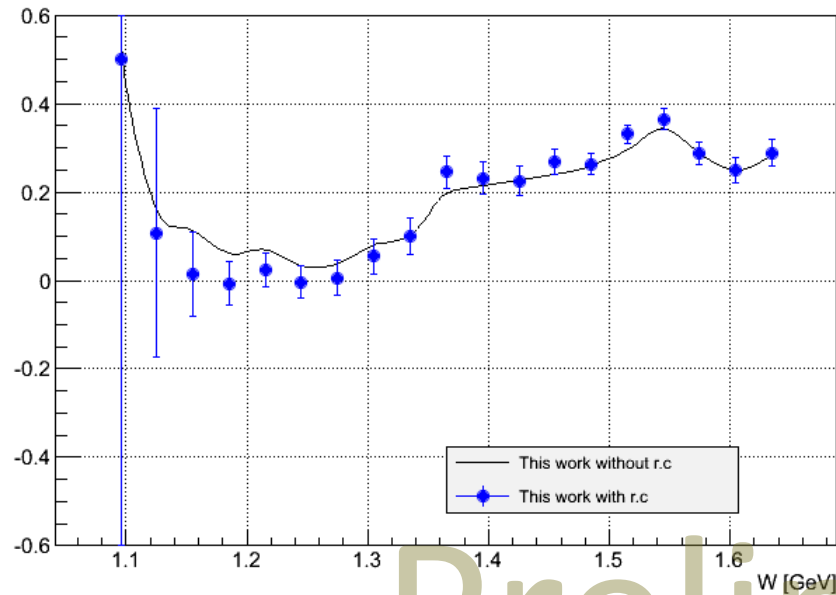
# HMS Asymmetries

Setting	Beam energy (GeV)	HMS central momentum (GeV)	HMS angle from beamline (degree)	$\langle Q^2 \rangle$ ( $GeV^2$ )	$\langle W \rangle$ (GeV)
(1)	4.7 (par) / 5.9 (per)	3.2 (par) / 4.4 (per)	20.2 (par) / 15.4 (per)	1.863	1.353
(2)	5.9	3.1	15.4	1.313	2.196
(3)	4.7	2.2	16	0.806	2.196

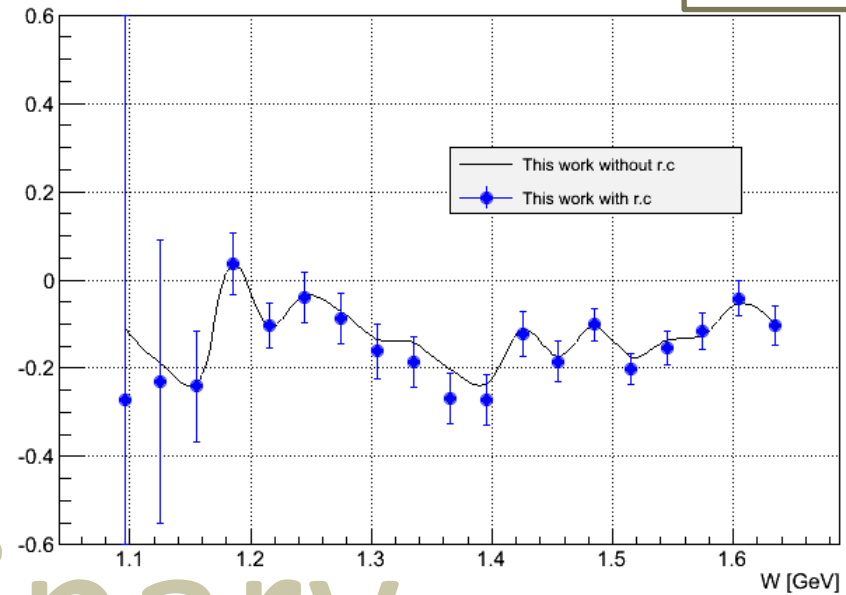
# Asymmetries with(out) radiative correction

$$Q^2 = 1.86 \text{ GeV}^2$$

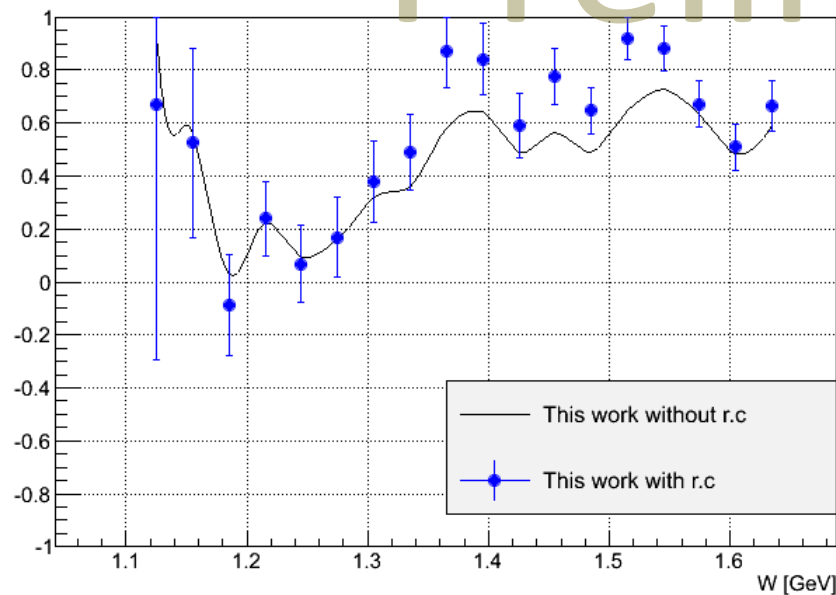
$A_{180}$  along W



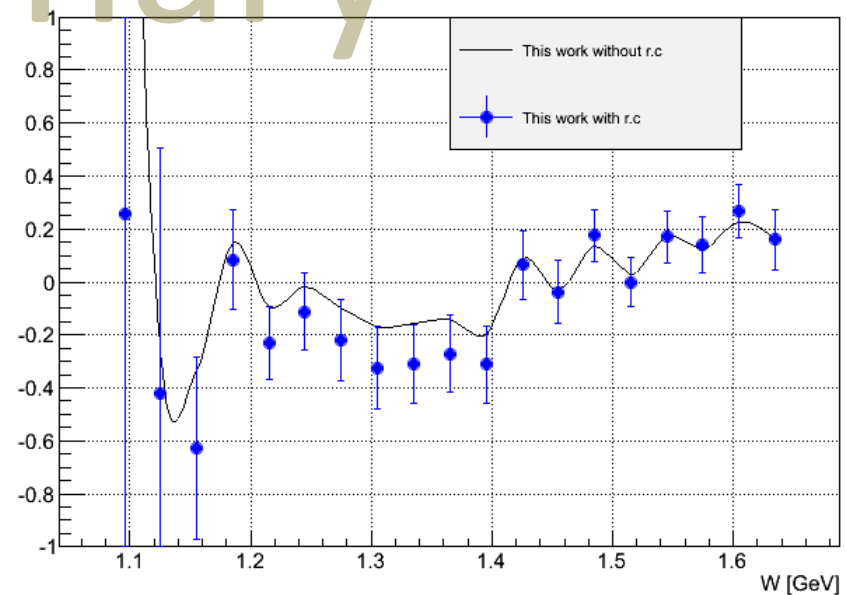
$A_{80}$  along W



$A_1$  along W



$A_2$  along W



# Asymmetries $A_1$ and $A_2$

$A_1$  and  $A_2$  are virtual photoabsorption asymmetries.

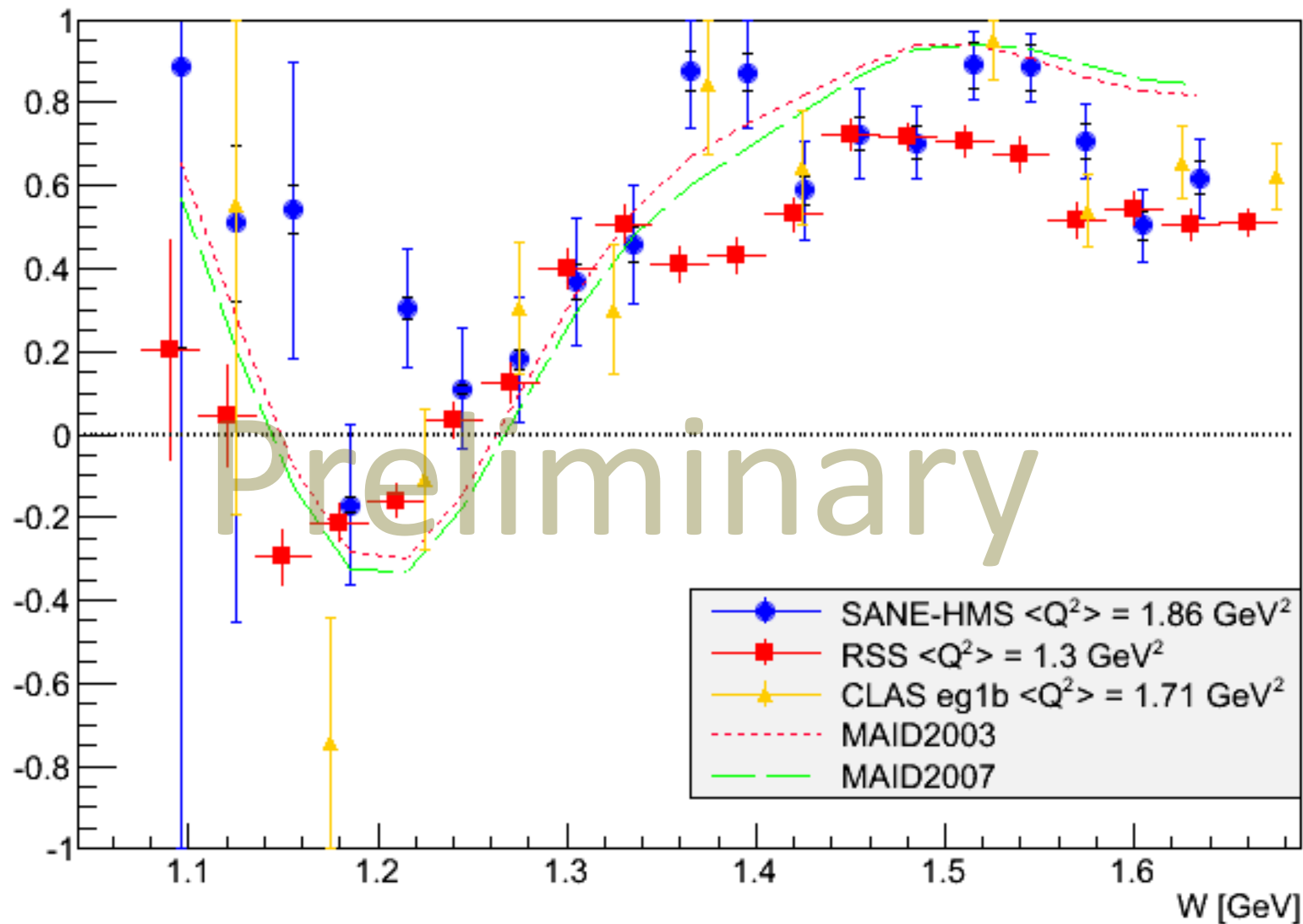
$$A_1 = \frac{\sigma_{1/2}^T - \sigma_{3/2}^T}{\sigma_{1/2}^T + \sigma_{3/2}^T} = \frac{\sigma_{TT}}{\sigma_T} = \frac{g_1 - \gamma^2 g_2}{F_1}$$
$$A_2 = \frac{2\sigma_{LT}}{\sigma_{1/2}^T + \sigma_{3/2}^T} = \frac{\sigma_{LT}}{\sigma_T} = \frac{\gamma(g_1 + g_2)}{F_1}$$

$\sigma_{1/2}^T$  and  $\sigma_{3/2}^T$  are the virtual photon absorption transverse cross sections when total helicity of photon and nucleon is 1/2 and 3/2 respectively.  $\sigma_{LT}$  is the interference term between the transverse and longitudinal photon-nucleon amplitude.

# Asymmetry $A_1 = \frac{\sigma_{TT}}{\sigma_T}$

$Q^2 = 1.86 \text{ GeV}^2$

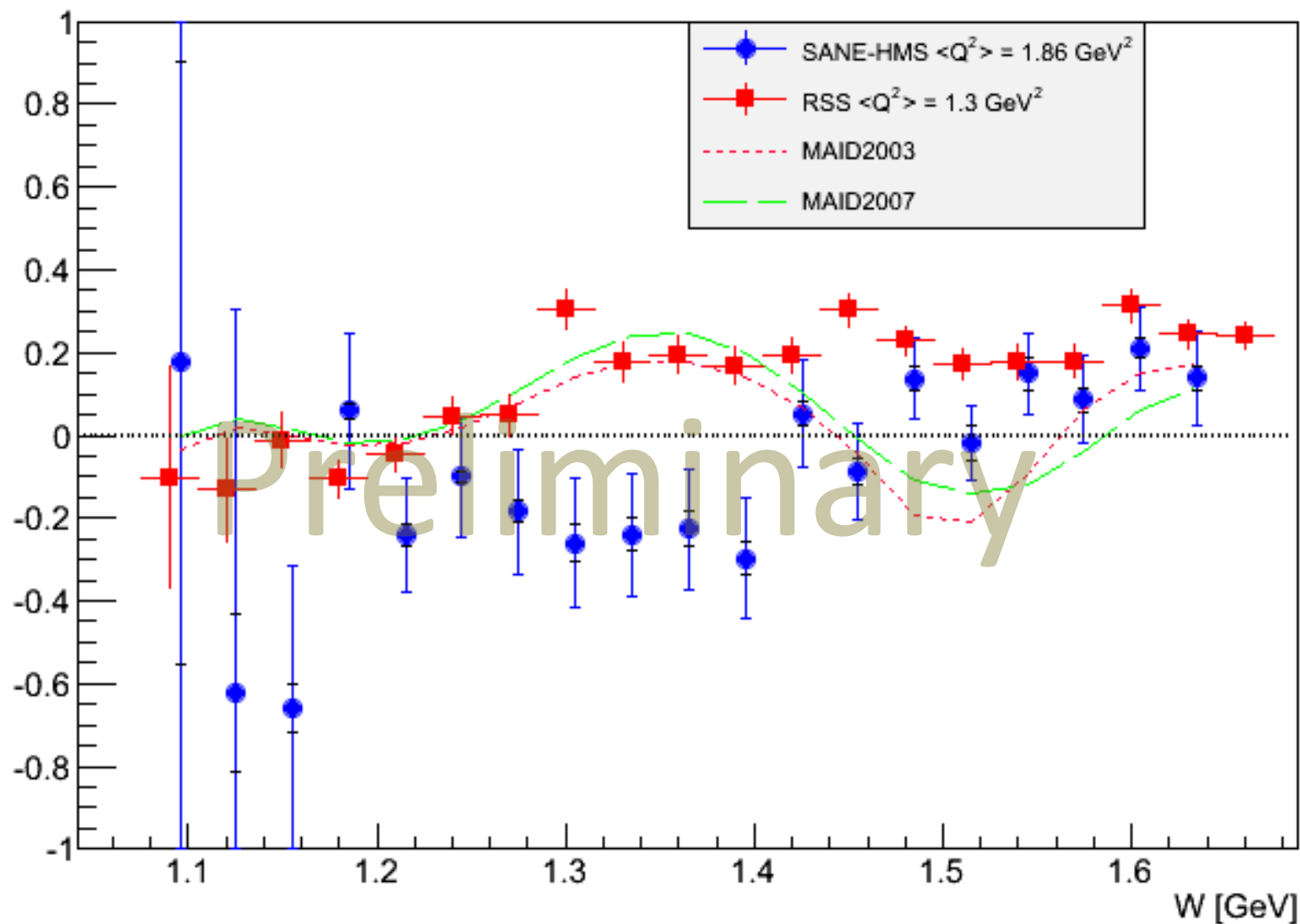
$A_1$  along W



$$\text{Asymmetry } A_2 = \frac{\sigma_{LT}}{\sigma_T}$$

$$Q^2 = 1.86 \text{ GeV}^2$$

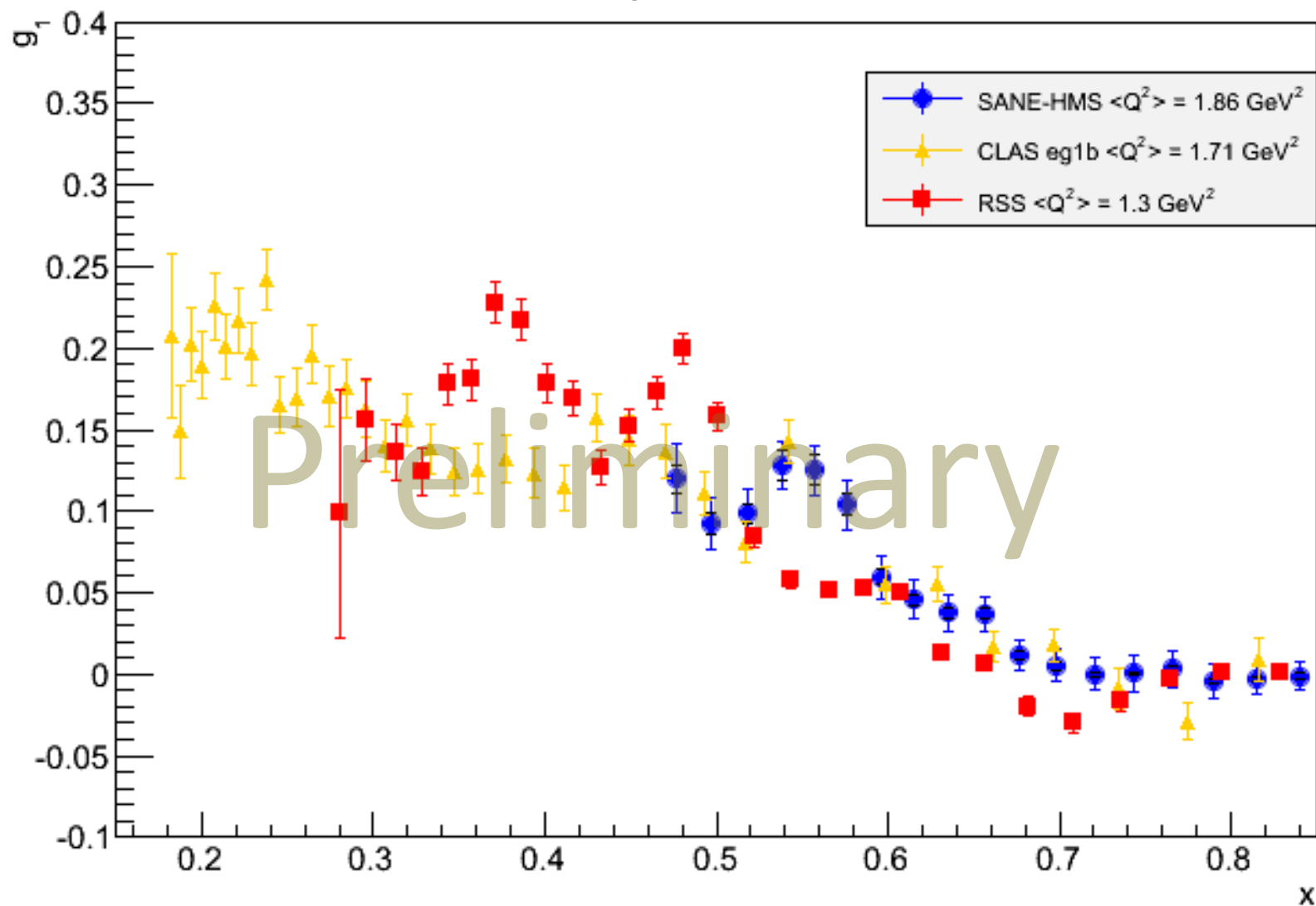
$A_2$  along W



# Structure Function $g_1$

$$Q^2 = 1.86 \text{ GeV}^2$$

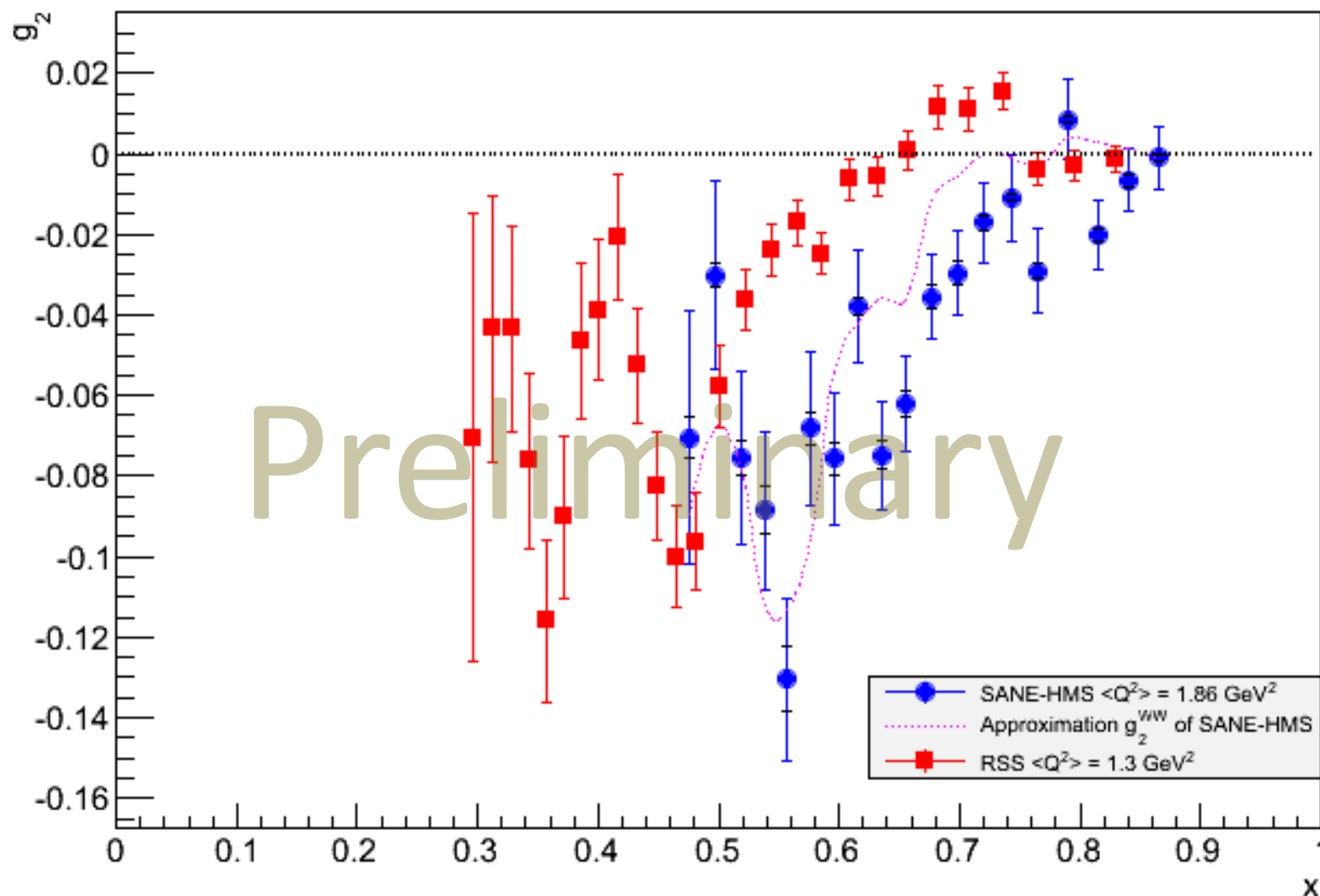
$g_1$  along x



# Structure Function $g_2$

$$Q^2 = 1.86 \text{ GeV}^2$$

$g_2$  along  $x$





# Twist-3 matrix element $d_2$

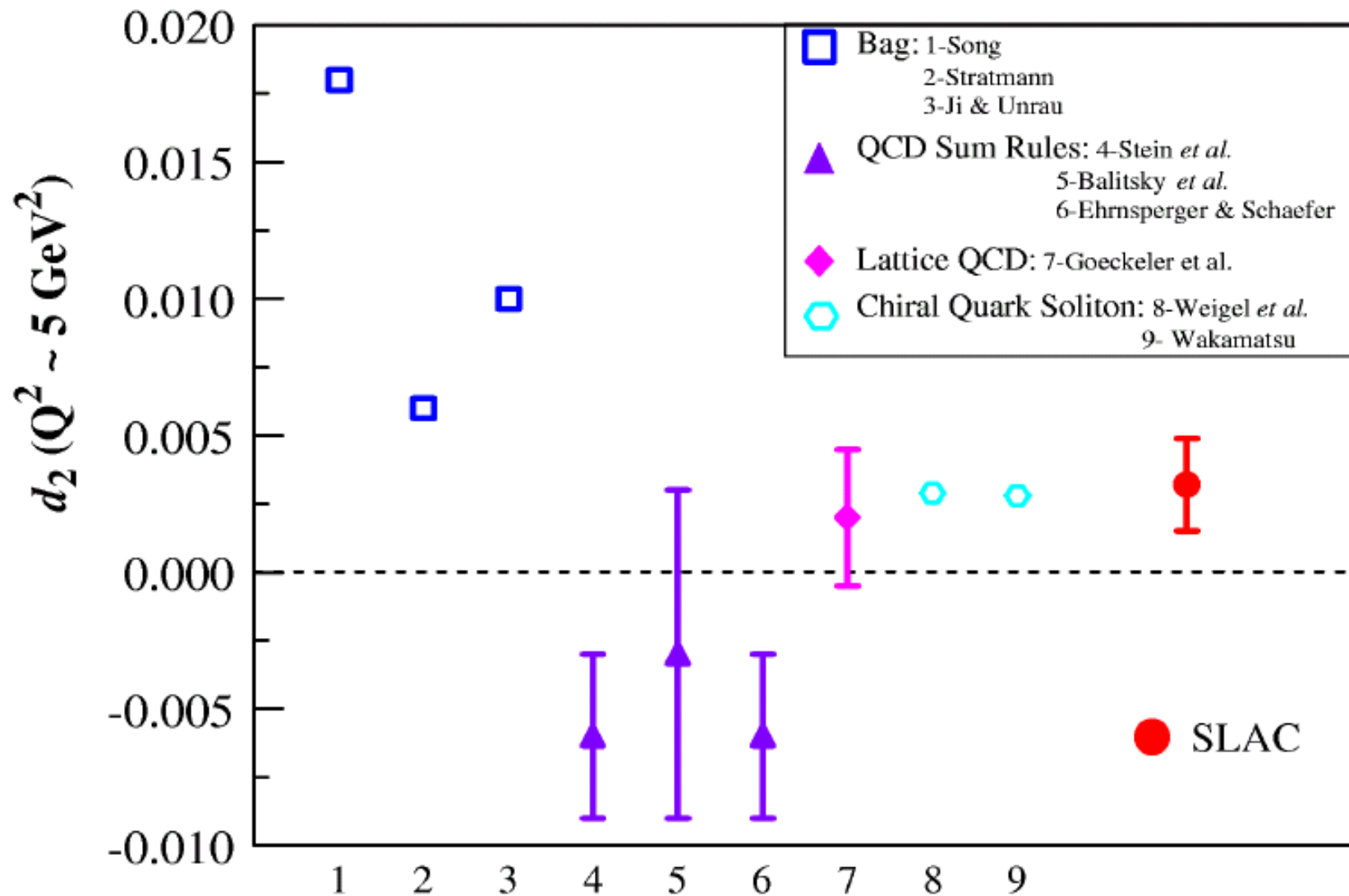
If we ignore higher twist effects,  $g_2$  is determined by  $g_1$ , using Wandzura-Wilczek relation:

$$g_2^{WW}(x, Q^2) = -g_1(x, Q^2) + \int_x^1 g_1(y, Q^2) \frac{dy}{y}$$

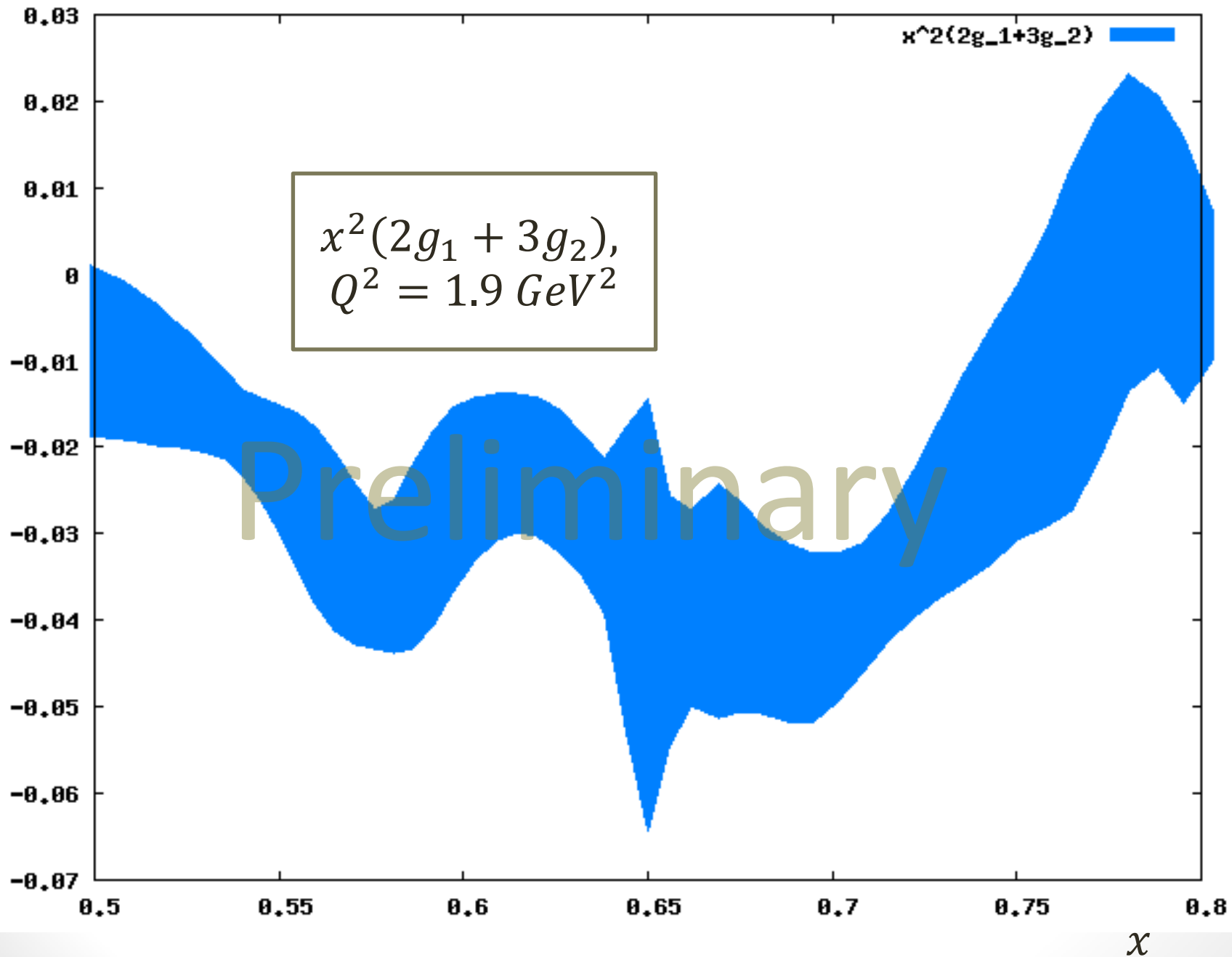
OPE relates the twist-3 matrix element  $d_2$  to the following:

$$d_2 = 3 \int_0^1 x^2 (g_2 - g_2^{WW}) dx = \int_0^1 x^2 (2g_1 + 3g_2) dx$$

# Twist-3 matrix element $d_2$



# Twist-3 matrix element $d_2$



## Twist-3 matrix element $d_2$

Very preliminary result of the limited  $x$  range is

$$\overline{d_2} = -0.0072 \pm 0.0004$$

$$\overline{d_2} = \int_{0.5}^{0.8} x^2 (2g_1 + 3g_2) dx$$

$A_1, A_2$  fit evaluated at  $Q^2 = 1.9 \text{ GeV}^2$

# **SANE collaboration**

**U. Basel, Florida International U., Hampton U.,  
Norfolk S. U., North Carolina A&T S. U., IHEP-  
Protvino, U. of Regina, Rensselaer Polytechnic I.,  
Rutgers U., Seoul National U., Temple U., TJNAF, U.  
of Virginia, College of William & Mary, Yerevan  
Physics I.**

**Spokespersons: S. Choi (Seoul), M. Jones(Jlab), Z-E.  
Meziani (Temple), O. A. Rondon (U. of Virginia)**

# Summary

- SANE-HMS data covers various kinematic regions and it can produce meaningful results, besides BETA(main detector) data.
- Preliminary spin asymmetry  $A_1$  and structure function  $g_1$  shows good agreement with previous experiments.
- But  $A_2$  and  $g_2$  show remarkable  $Q^2$  dependency.
- Preliminary twist-3 matrix element  $d_2$  of the limited x range is  $-0.0072 \pm 0.0004$ .
- World first proton transverse spin data on this kinematic region is expected to improve global fits.

**Backup slides**

# Experimental goal

The goal is to get the proton spin structure functions  $g_1$  and  $g_2$  over broad range of the Bjorken scaling variable

$$0.3 \leq x \leq 0.8$$

and 4-momentum transfer

$$2.5 \text{GeV}^2 \leq Q^2 \leq 6.5 \text{GeV}^2$$

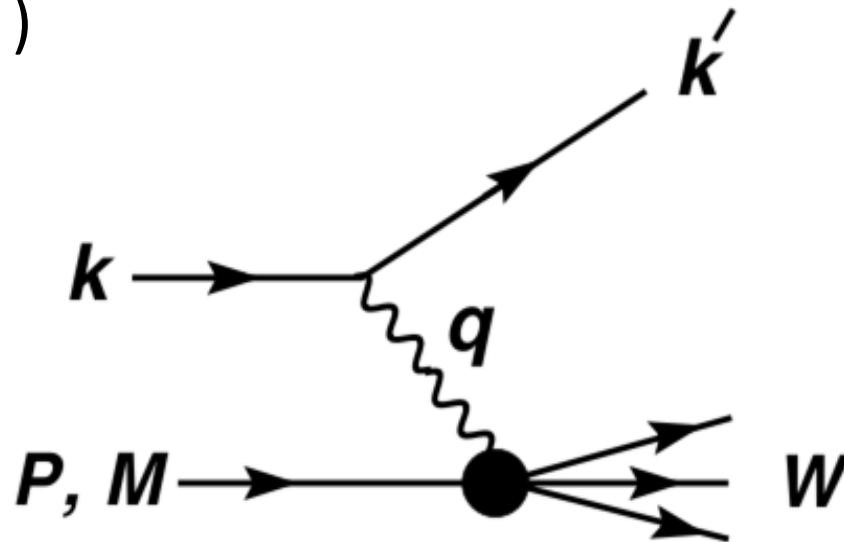


# ep deep inelastic scattering

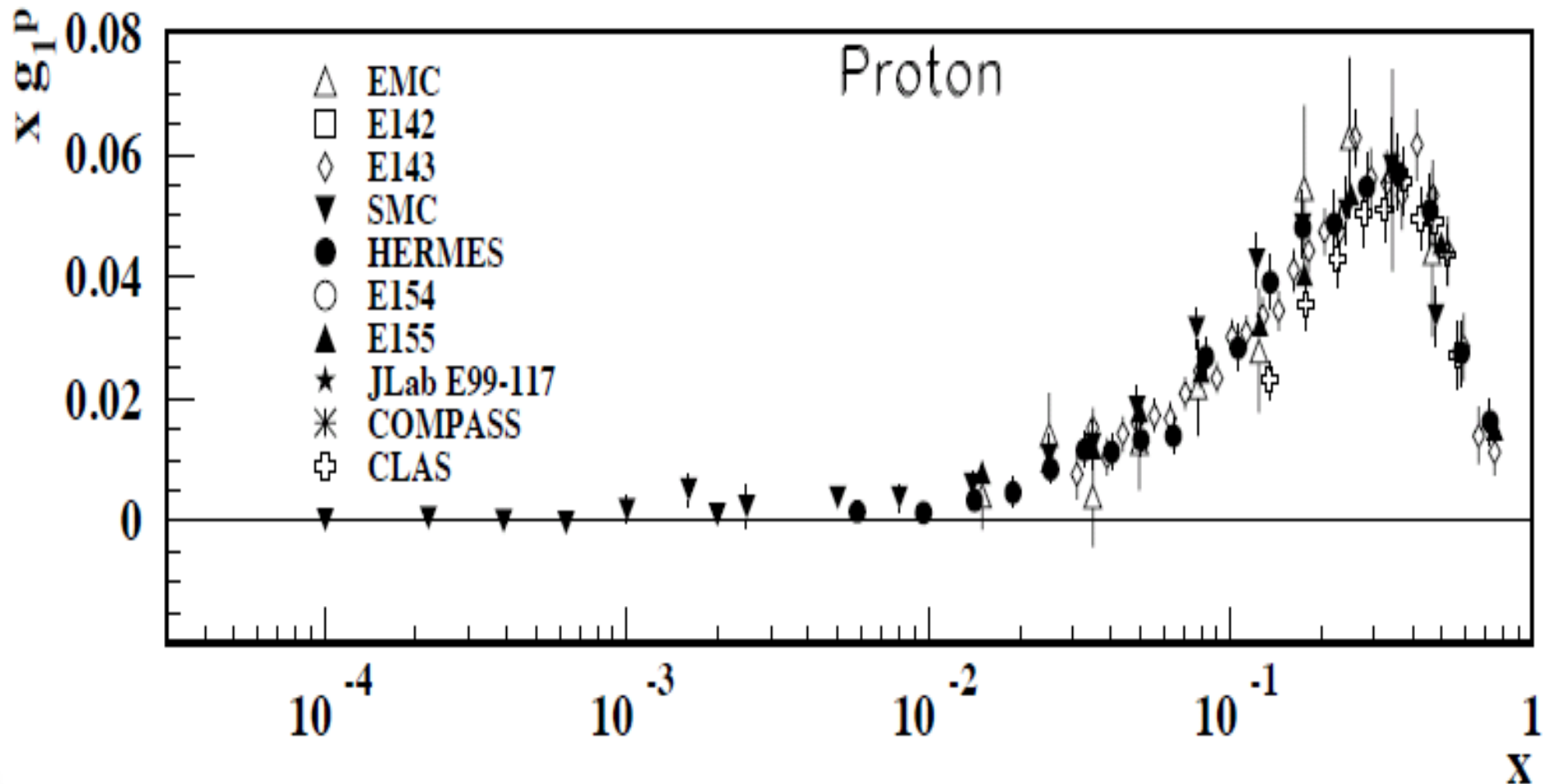
High-energy electron-nucleon scattering (Deep Inelastic Scattering)  $ep \rightarrow e'X$

$k$  and  $k'$  are the four-momenta of the incoming and outgoing electrons,  $P$  is the four-momentum of a proton with mass  $M$ , and  $W$  is the mass of the recoiling system  $X$ .

$q$  is the four-momentum of the virtual photon (the exchanged particle). ( $Q^2 = -q^2$ )



# World Data of $g_1$



# Jefferson Lab

## Thomas Jefferson National Accelerator Facility



Located in Newport News,  
Virginia, USA

Funded by the U.S. Department  
of Energy's Office of Science

Having CEBAF (Continuous  
Electron Beam Accelerator Facility)  
and three experimental halls

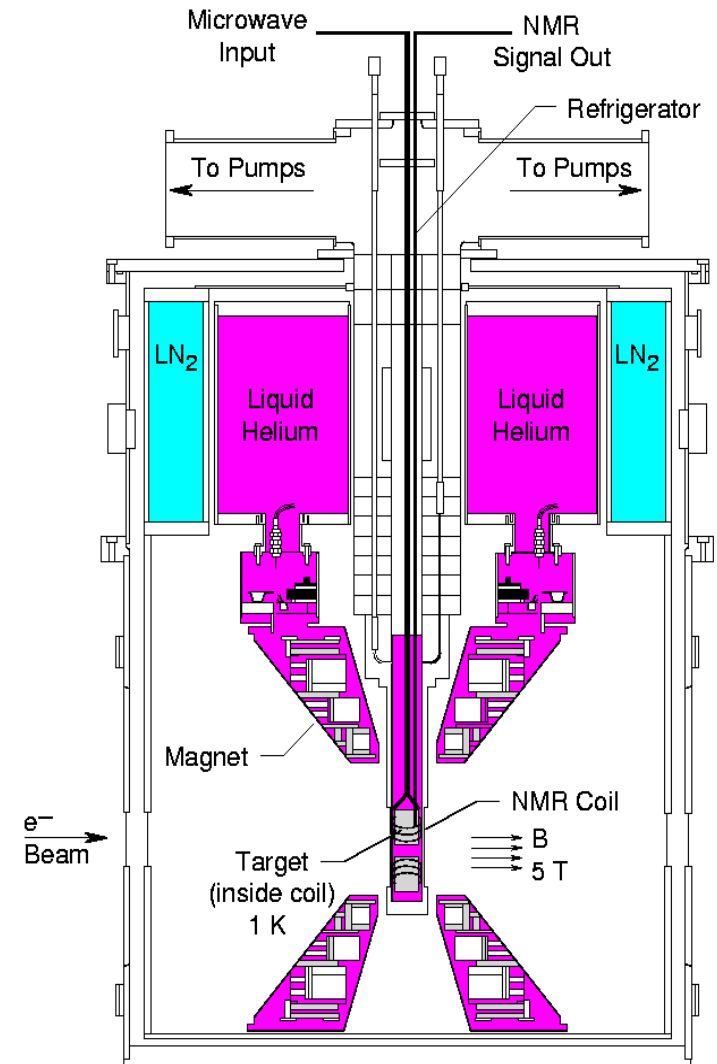


# UVA Target

Superconducting magnet  
applies 5-T magnetic field.

The target and the magnet  
are cooled down by liquid  
helium.

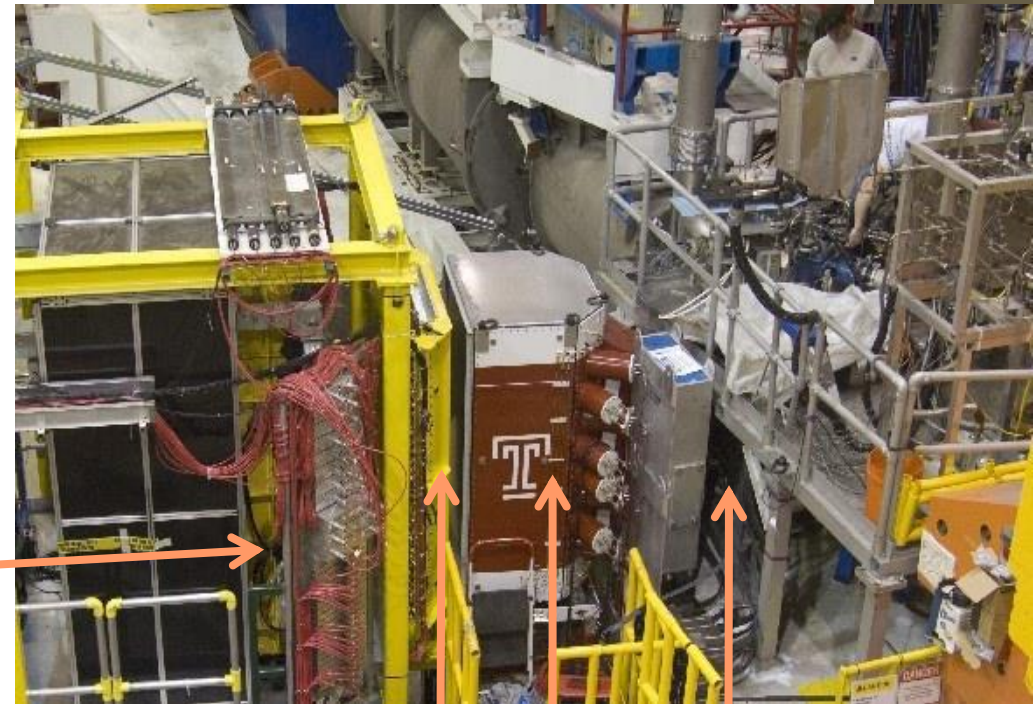
~140 Ghz microwave  
frequency causes dynamic  
nuclear polarization up to  
90%.





# Big Electron Telescope Array - BETA

- **BigCal** lead glass calorimeter:  
main detector, being built for *GEp-III*.
- **Gas Cherenkov**: additional pion rejection
- Tracking **Lucite hodoscope**
- BETA's characteristics
  - Effective solid angle = 0.194 sr
  - Energy resolution  $5\%/\sqrt{E(\text{GeV})}$
  - angular resolution  $< 0.8^\circ$
  - 1000:1 pion rejection
- Added: **forward hodoscope**
  - vertex resolution  $\sim 5$  mm
  - angular resolution  $\sim 1$  mr
- Target field sweeps low  $E$  background



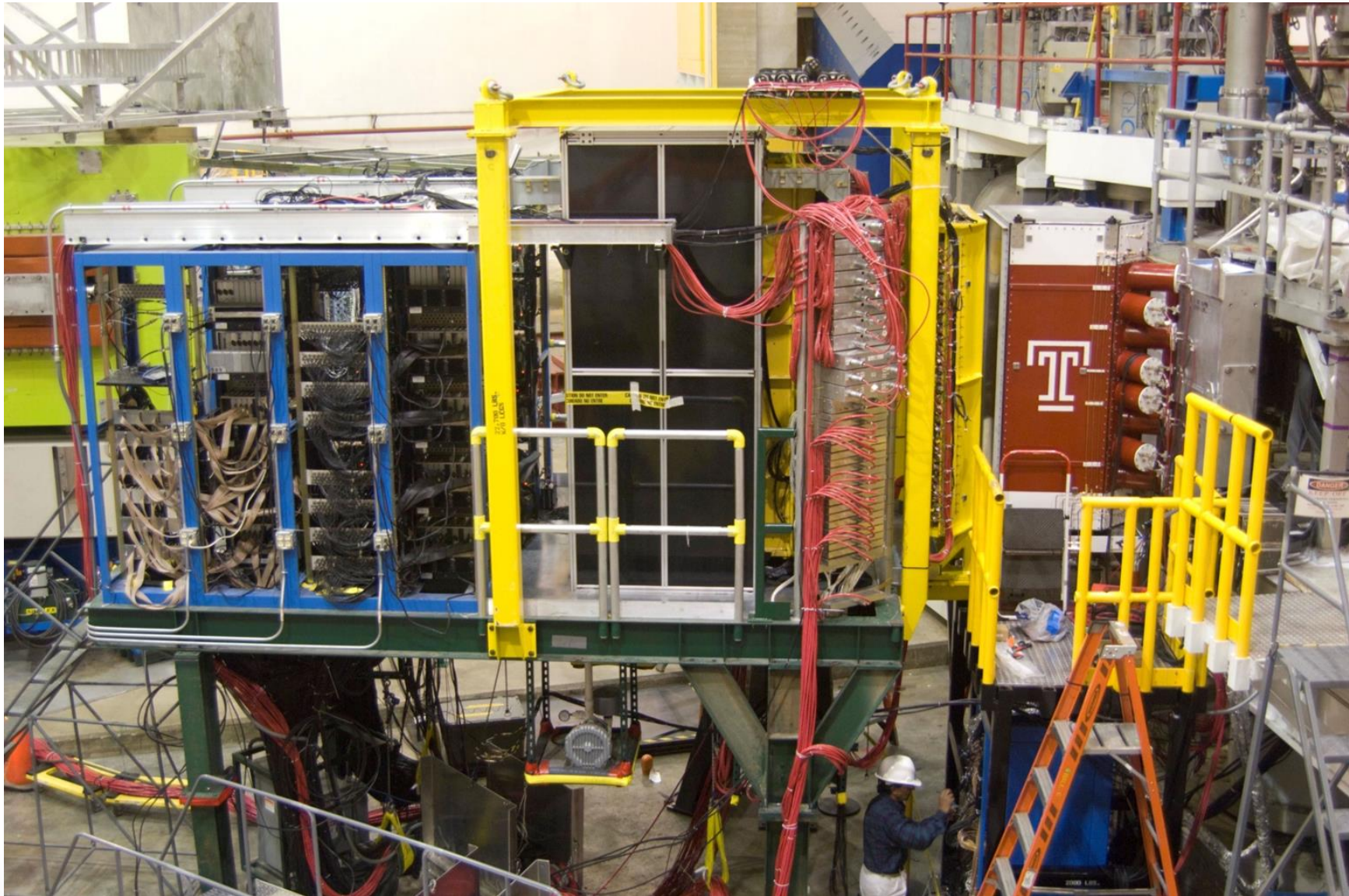
**BigCal**

**Lucite Hodoscope**

**Tracker**

**Cherenkov**

# BETA

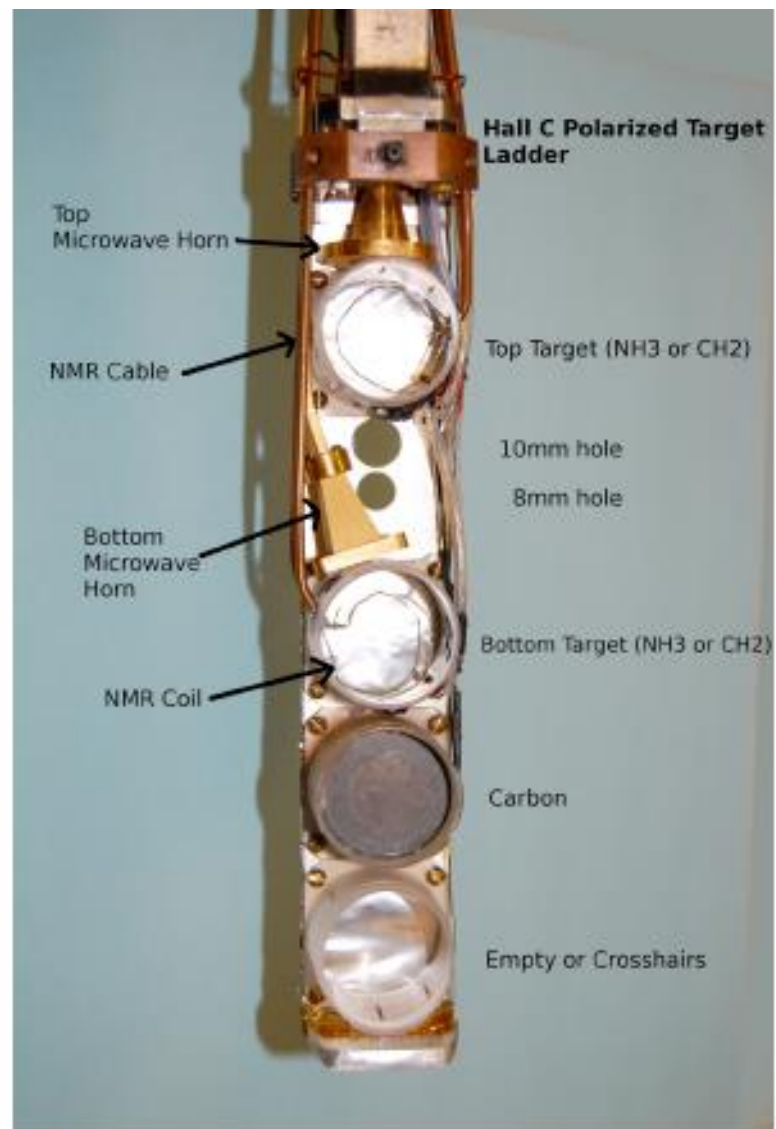




# Target insert



$\text{NH}_3$

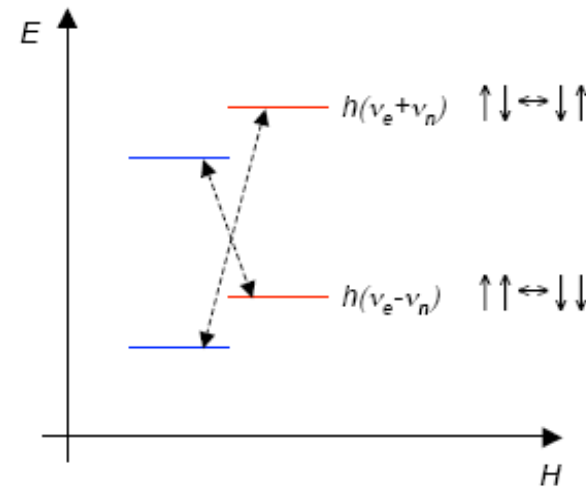
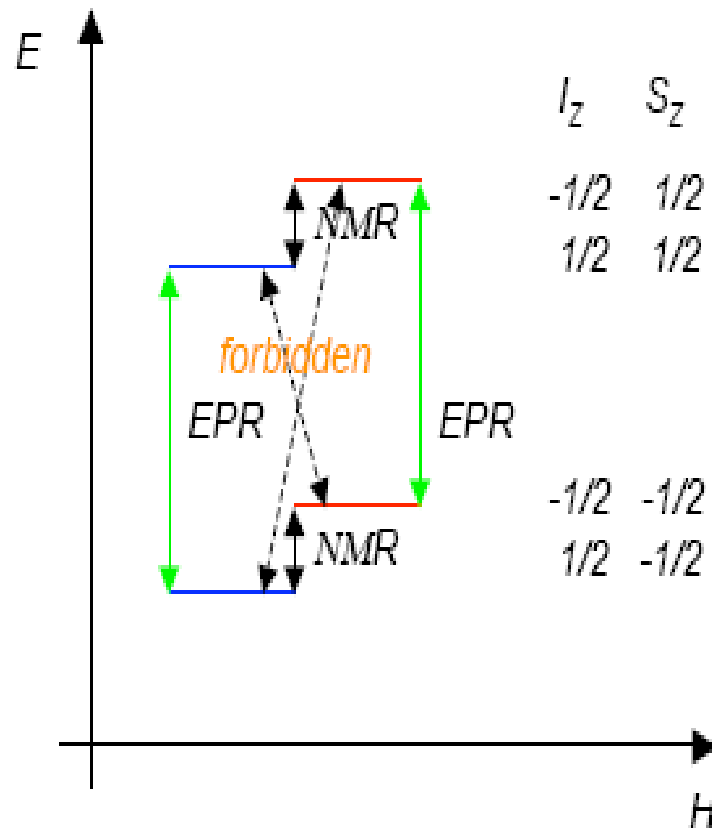


# Dynamic Nuclear Polarization

The DNP process for polarizing protons, deuterons, or any nucleus possessing a magnetic moment, requires temperatures of  $\leq 1$  K or less and large magnetic holding fields. For thermal equilibrium at 1 K and 5 T, the proton polarization is only about 0.5%. However, the polarization of the “free” electrons, associated with the paramagnetic radicals introduced into the target material, is greater than 99%. The electron polarization can be transferred to the proton through a hyperfine transition by irradiating the target with microwaves at appropriate frequencies.



# Dynamic Nuclear Polarization



The rf field drives the forbidden transitions.

flip-flops:  $\uparrow\downarrow \leftrightarrow \downarrow\uparrow$

flip-flips:  $\uparrow\uparrow \leftrightarrow \downarrow\downarrow$

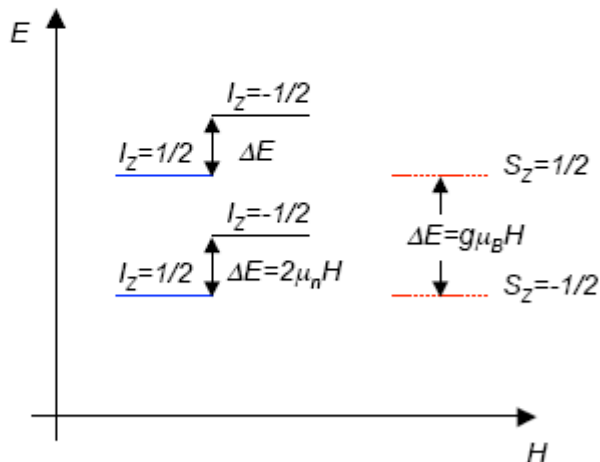
$$\Delta(S_z + I_z) = 0, 2$$

# Dynamic Nuclear Polarization

Nucleons also possess magnetic moment, although:

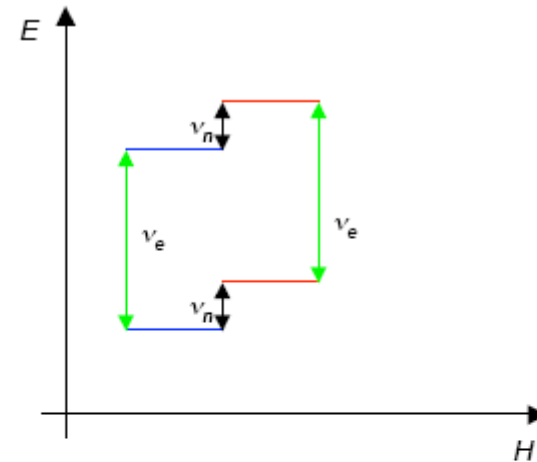
Nuclear moments/Electron Moments  $\sim 10^{-3}$

Including nuclear moments  $\Rightarrow$  Hyperfine Splitting



$S_z$ : Electrons

$I_z$ : Nucleons, Nuclei



1)  $\nu_{rf} \sim \nu_e$  get transitions  $-- \rightarrow -+$   
 $++ \rightarrow +-$   
 where  $\Delta E = g\mu_B H = h\nu_e$

2)  $\nu_{rf} \sim \nu_n$  get transitions  $+- \rightarrow ++$   
 $++ \rightarrow -+$   
 where  $\Delta E = 2\mu_n H = h\nu_n$

# Dilution Factor from Packing Fraction

Total yield has linear relation with packing fraction:

$$Y_T = m pf + b$$

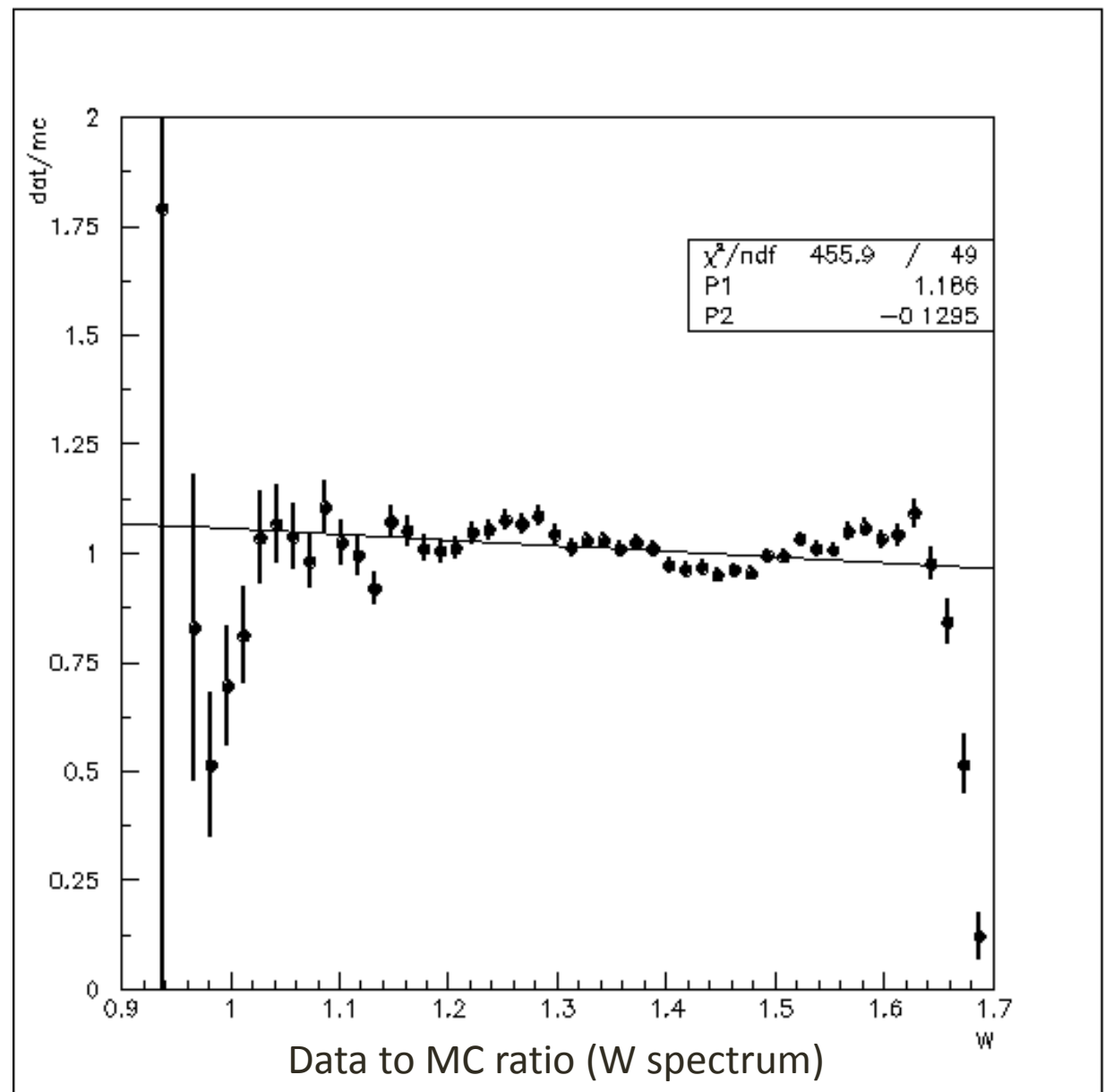
Using MC (P. E. Bosted and M. E. Christy, Phys. Rev., C 77, 065206 (2008))

assuming two different  $pf$ , the slope( $m$ ) and intercept( $b$ ) can be calculated and then the yield of real data produces  $pf$  of real target.

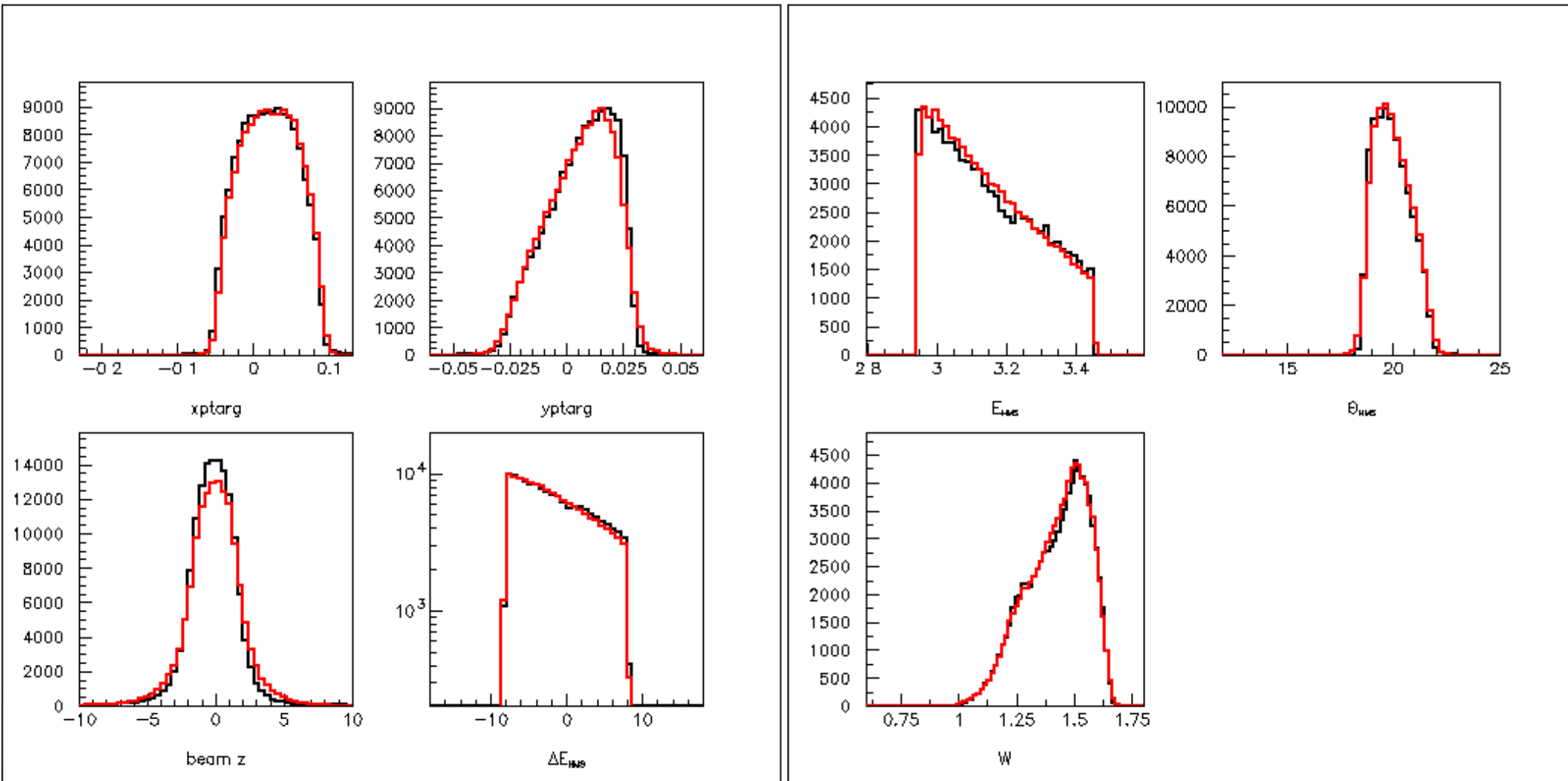
SANE packing fractions are 56% - 62% with  $\sim 4.5\%$  error.

# Packing Fraction

Comparing data with Monte Carlo results assuming 50% and 60% packing fraction of target, 60.9% packing fraction is determined for the target material #9 6-28-07 14NH3.



# Packing Fraction



Data and MC comparison (Red is MC)

# Fitting Function

$$\text{fit} = \underbrace{\sum_{i=1}^4 BW_i}_{\text{Resonances}} + \underbrace{x^\alpha \sum_{n=0}^3 \beta_n x^n}_{\text{DIS}} \times \underbrace{\frac{1}{\sqrt{Q^2}}}_{A_2 \text{ only}}$$

where

$$BW_i = \frac{a_i \kappa_i^2 w_i^2 \Gamma_i \Gamma_i^\gamma}{\kappa_{cm}^2 [(w_i^2 - W^2)^2 + w_i^2 \Gamma_i^2]}$$

$$\begin{aligned} &= g_i \left( \frac{q_{cm}}{q_i} \right)^{(2l_i+1)} \left( \frac{q_i^2 + X_i^2}{q_{cm}^2 + X_i^2} \right)^{l_i} \\ &= g_i \left( \frac{\kappa_{cm}}{\kappa_i} \right)^{(2j_i)} \left( \frac{\kappa_i^2 + X_i^2}{\kappa_{cm}^2 + X_i^2} \right)^{j_i} \end{aligned}$$

$$\kappa_i = \sqrt{\frac{(w_i^2 + M^2 + Q^2)^2}{4w_i^2} - M^2}$$

$$q_i = \sqrt{\frac{(w_i^2 + M^2 - m_\pi^2)^2}{4w_i^2} - M^2}$$

$$\kappa_{cm} = \sqrt{\frac{(W^2 + M^2 + Q^2)^2}{4W^2} - M^2}$$

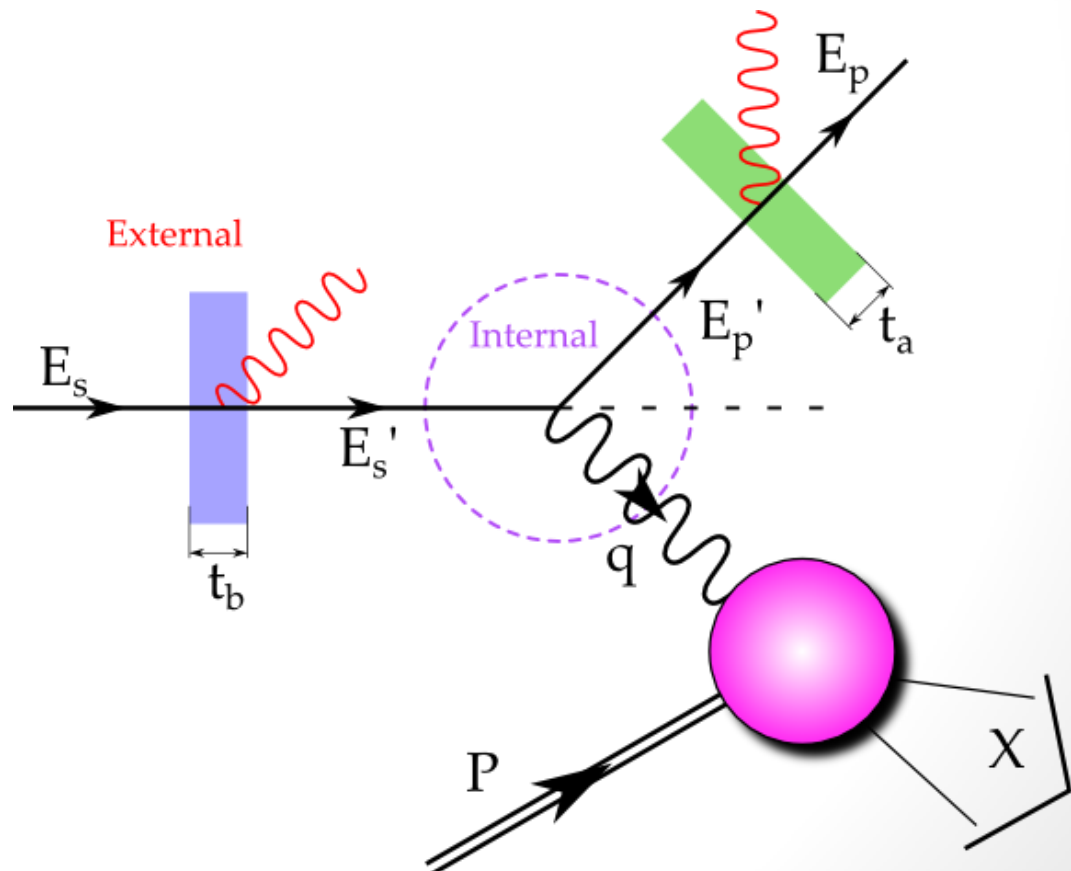
$$q_{cm} = \sqrt{\frac{(W^2 + M^2 - m_\pi^2)^2}{4W^2} - M^2}$$

# Radiative Correction

$$A = \frac{1}{f C_N P_b P_t f_{RC}} \frac{d\sigma^{\downarrow\uparrow} - d\sigma^{\uparrow\uparrow}}{d\sigma^{\downarrow\uparrow} + d\sigma^{\uparrow\uparrow}} + A_{RC}$$

Radiative Correction

1. Incoming and outgoing electron lose energy before and after scattering.
2. Elastic tail should be subtracted.
3. QED processes other than Born contributes to data.



# ep deep inelastic scattering

Invariant quantities:

$\nu = \frac{q \cdot P}{M} = E - E'$  is the lepton's energy loss in the nucleon rest frame (in earlier literature sometimes  $\nu = q \cdot P$ ). Here,  $E$  and  $E'$  are the initial and final lepton energies in the nucleon rest frame.

$Q^2 = -q^2 = 2(EE' - \vec{k} \cdot \vec{k}') - m_\ell^2 - m_{\ell'}^2$ , where  $m_\ell(m_{\ell'})$  is the initial (final) lepton mass.  
If  $EE' \sin^2(\theta/2) \gg m_\ell^2, m_{\ell'}^2$ , then

$\approx 4EE' \sin^2(\theta/2)$ , where  $\theta$  is the lepton's scattering angle with respect to the lepton beam direction.

$x = \frac{Q^2}{2M\nu}$  where, in the parton model,  $x$  is the fraction of the nucleon's momentum carried by the struck quark.

$y = \frac{q \cdot P}{k \cdot P} = \frac{\nu}{E}$  is the fraction of the lepton's energy lost in the nucleon rest frame.

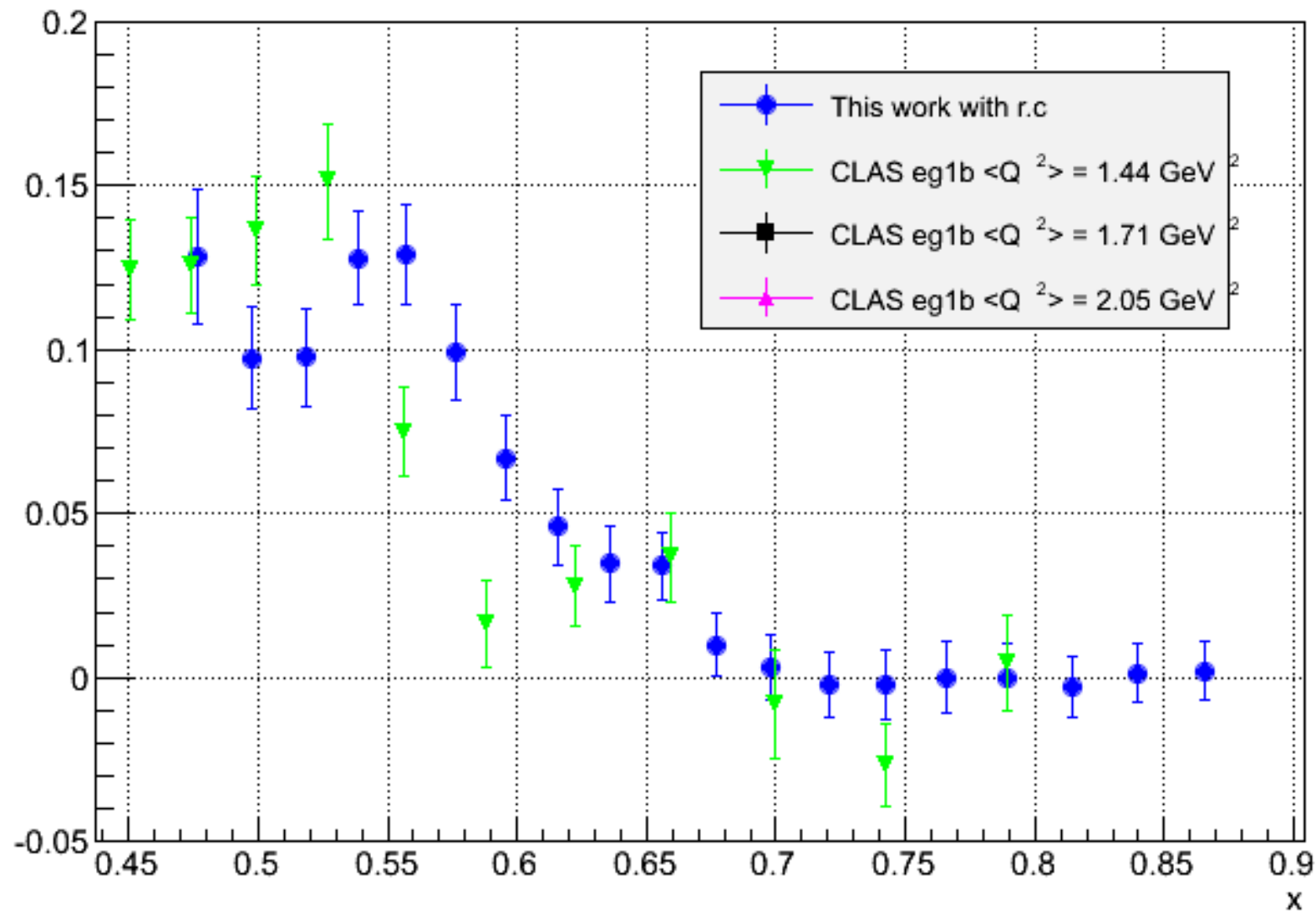
$W^2 = (P + q)^2 = M^2 + 2M\nu - Q^2$  is the mass squared of the system  $X$  recoiling against the scattered lepton.



# Structure Function $g_1$

$$Q^2 = 1.86 \text{ GeV}^2$$

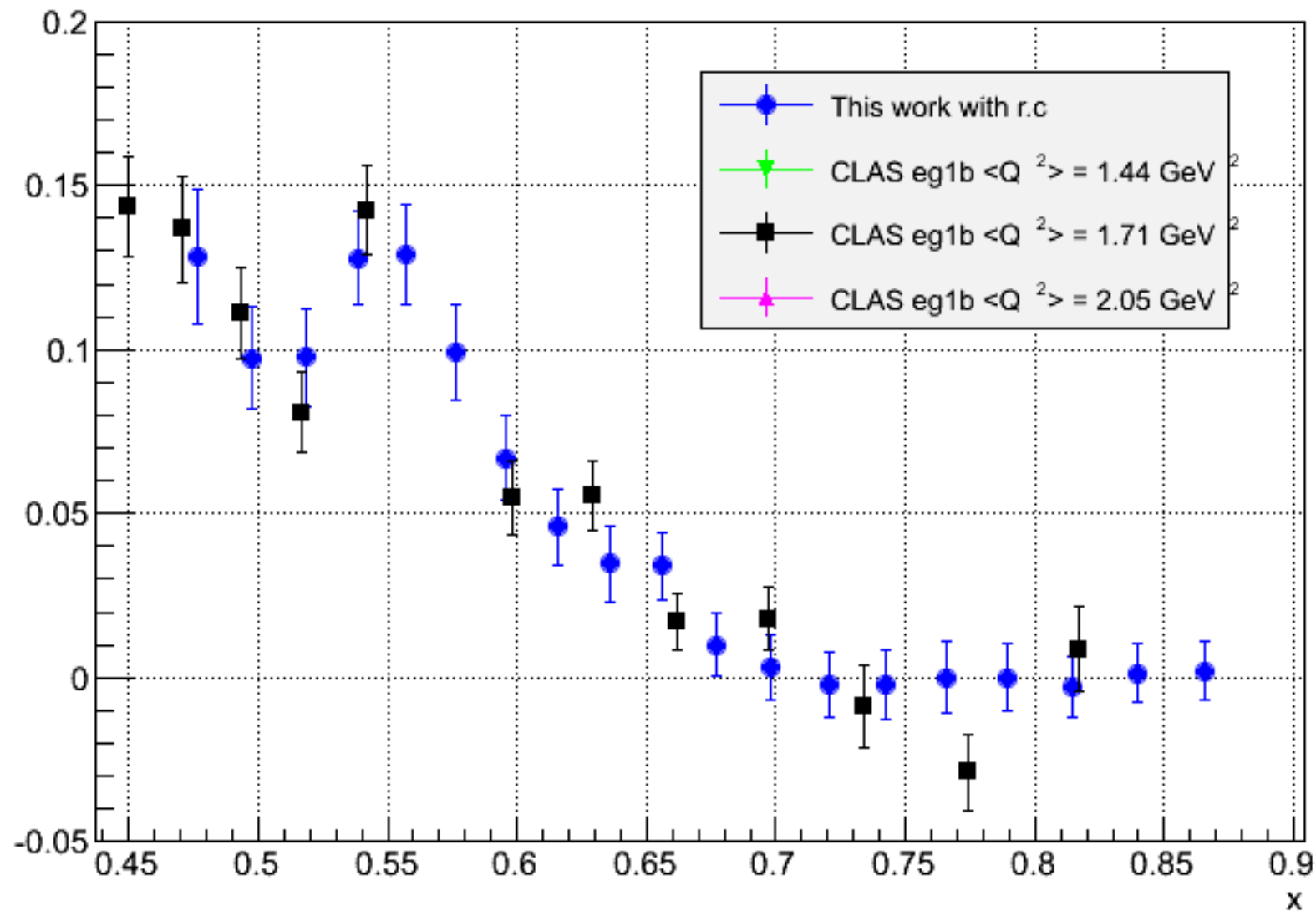
$g_1$  along x



# Structure Function $g_1$

$$Q^2 = 1.86 \text{ GeV}^2$$

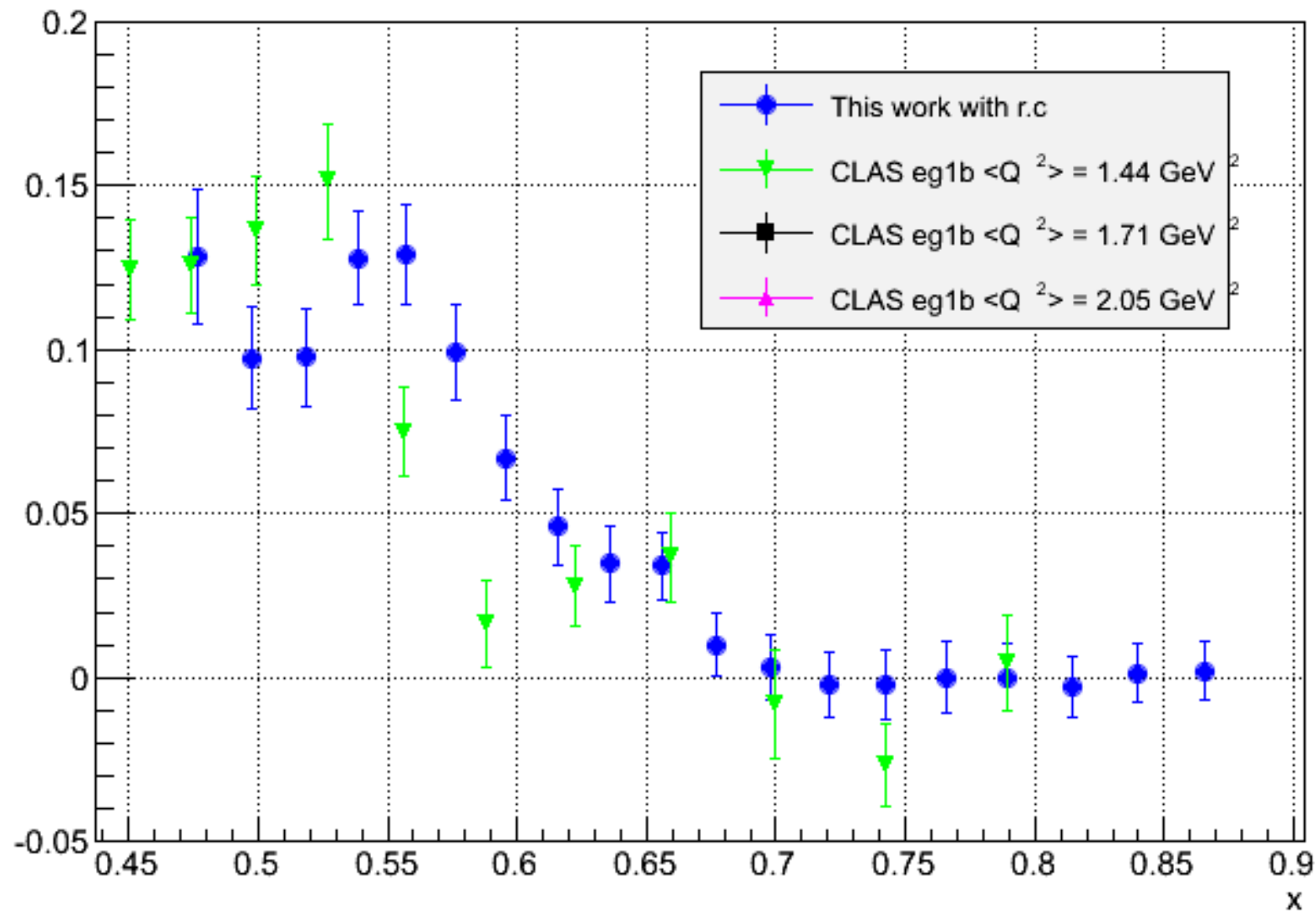
$g_1$  along x



# Structure Function $g_1$

$$Q^2 = 1.86 \text{ GeV}^2$$

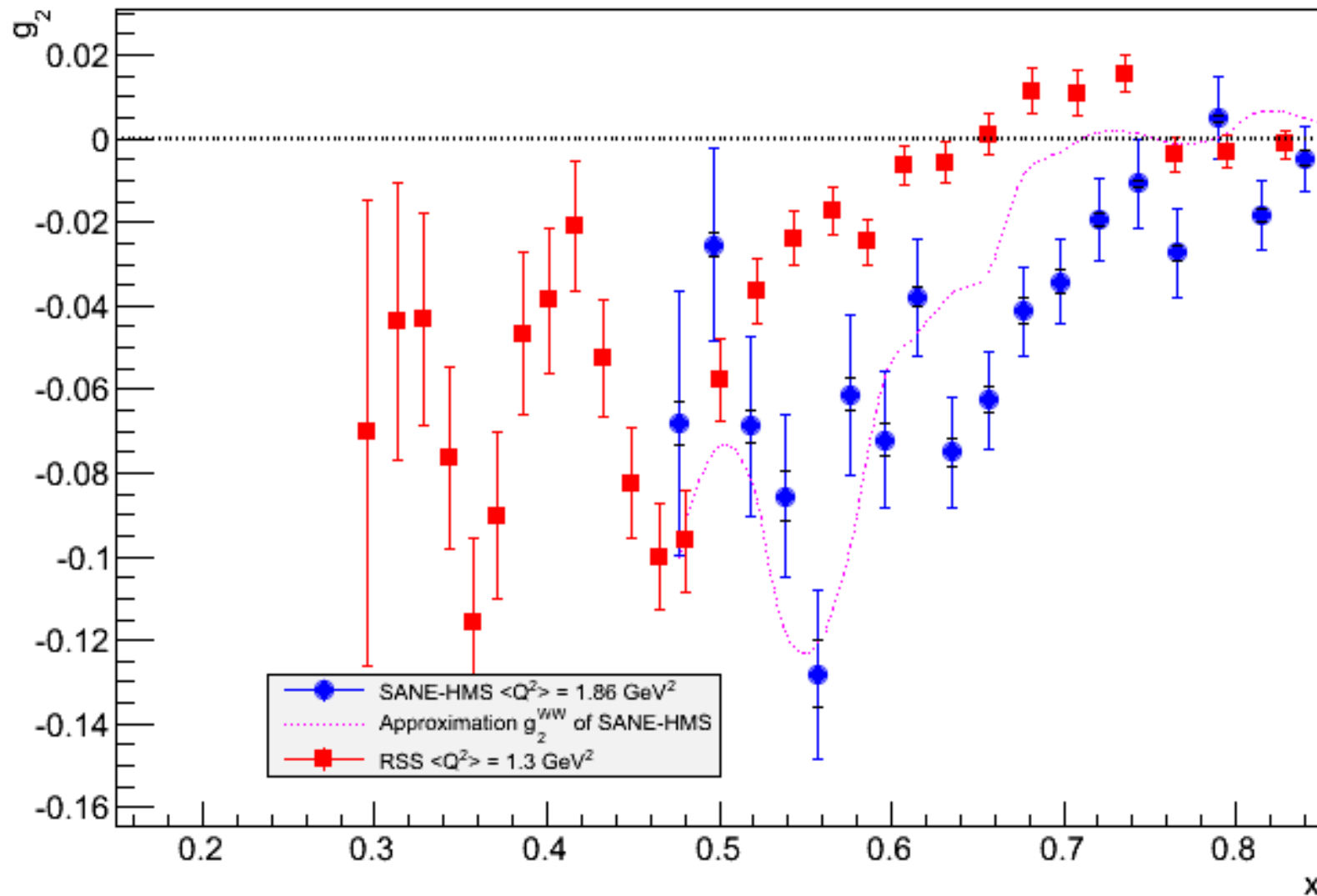
$g_1$  along x



# Structure Function $g_2$

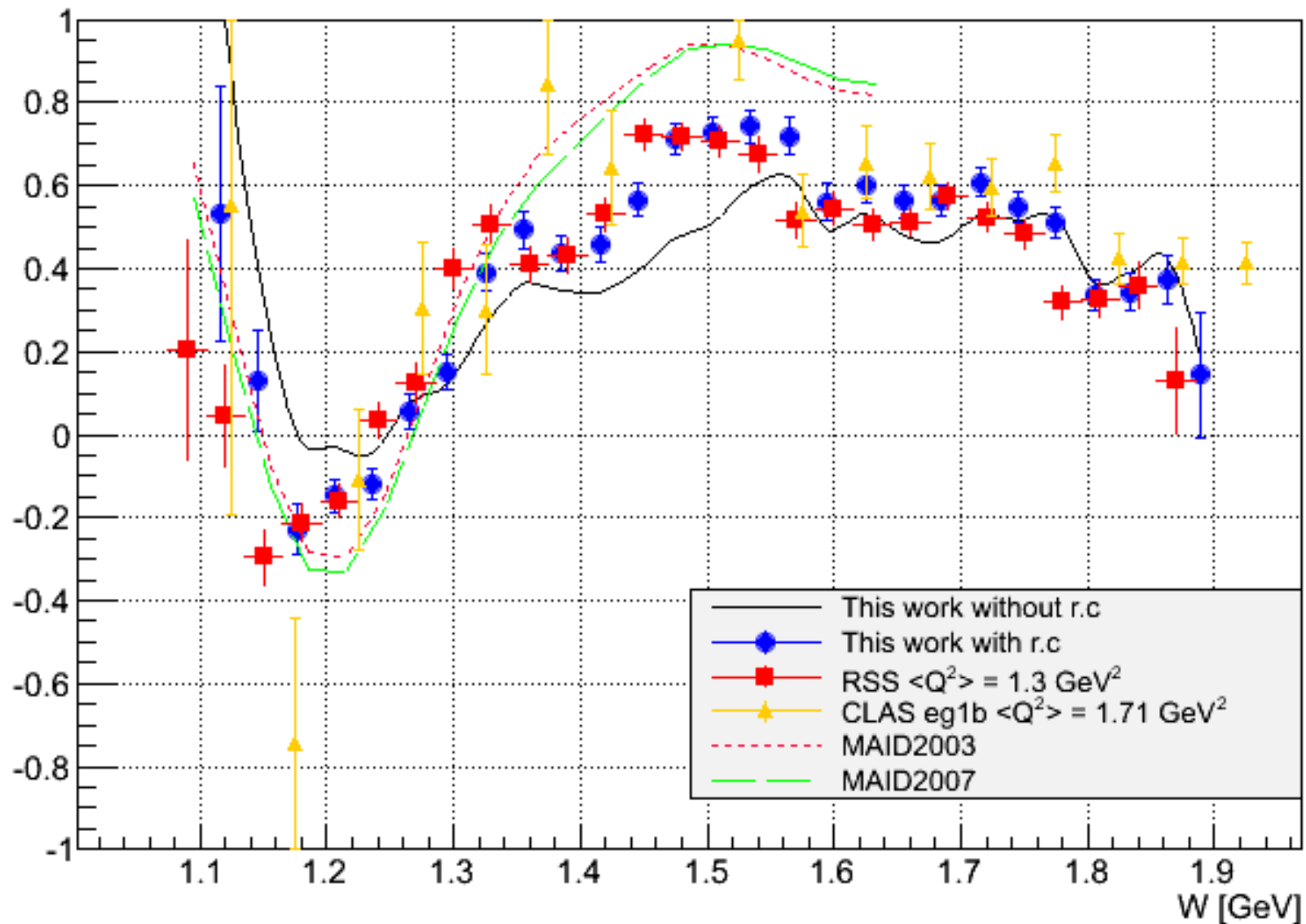
$$Q^2 = 1.86 \text{ GeV}^2$$

$g_2$  along  $x$

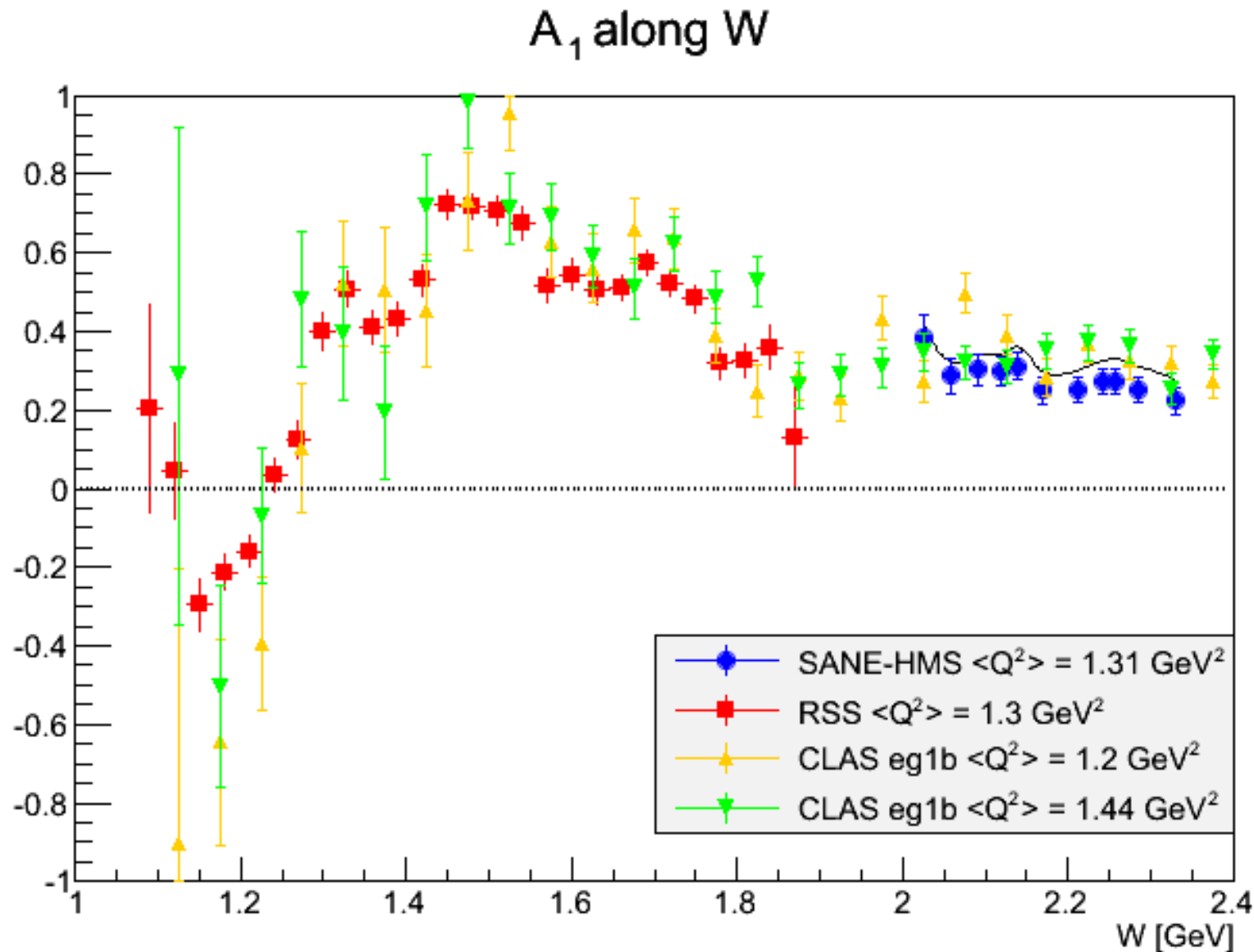


# Regenerated RSS result

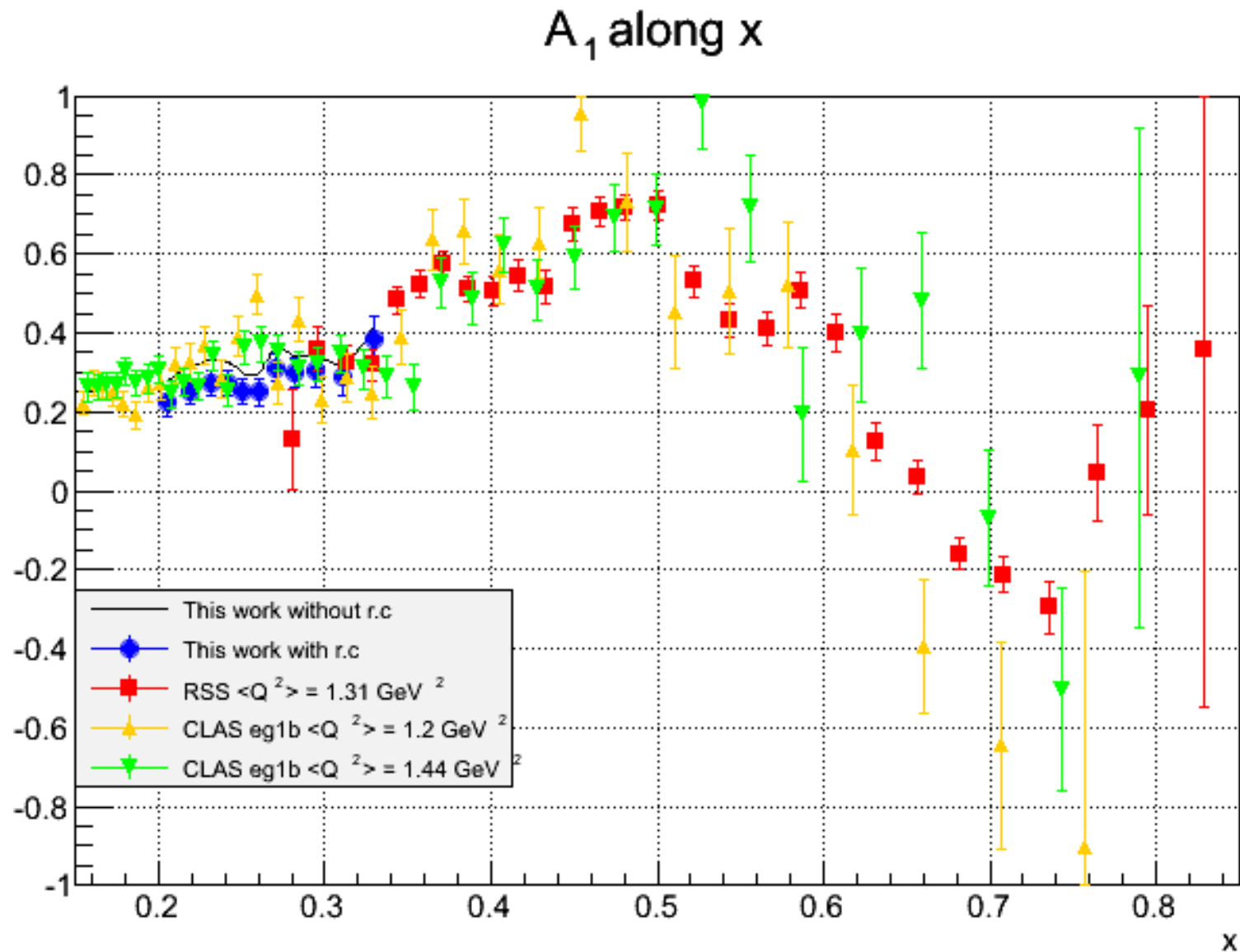
$A_1$  along  $W$



# Continuity with RSS and CLAS

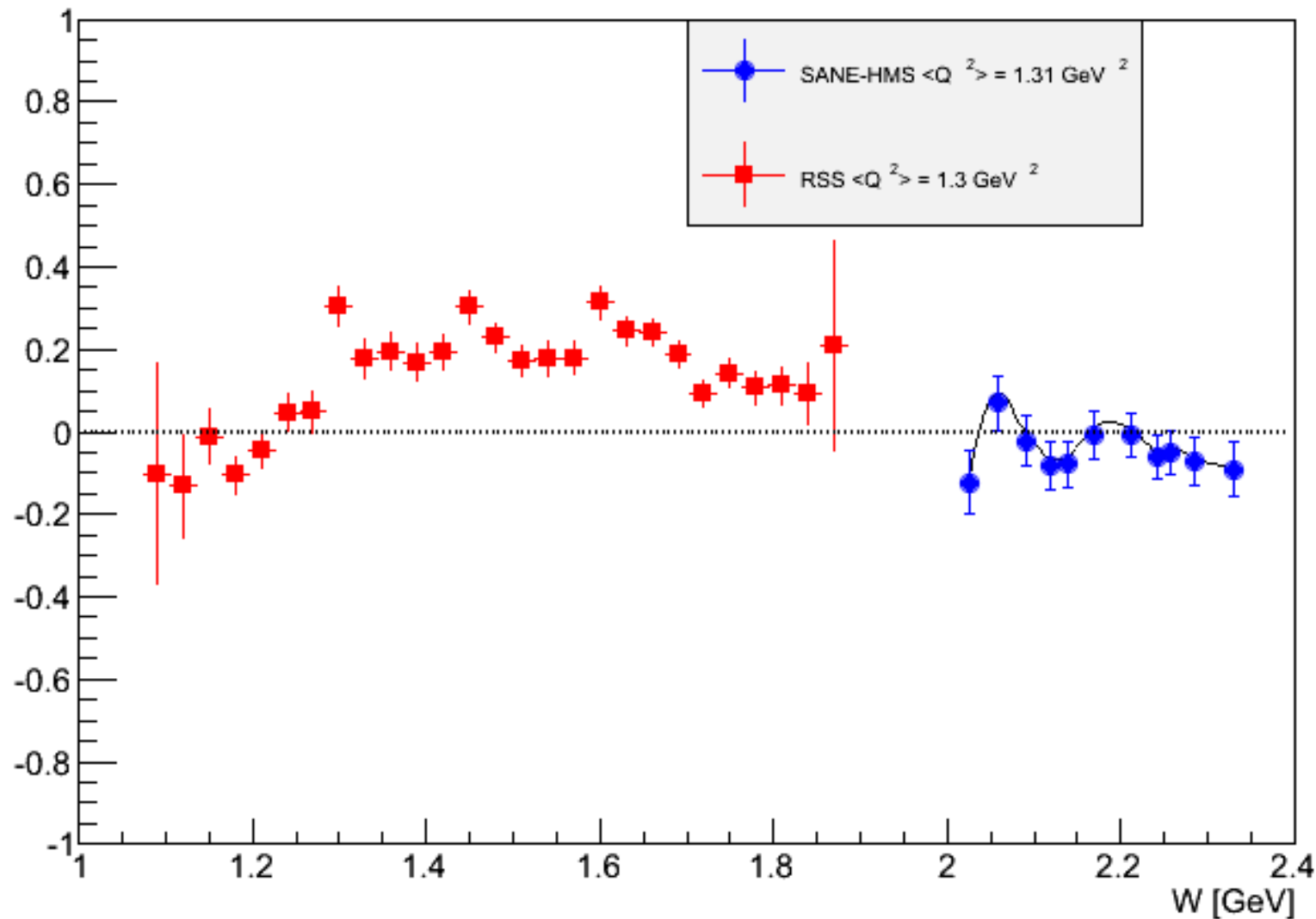


# Continuity with RSS and CLAS



# Continuity with RSS

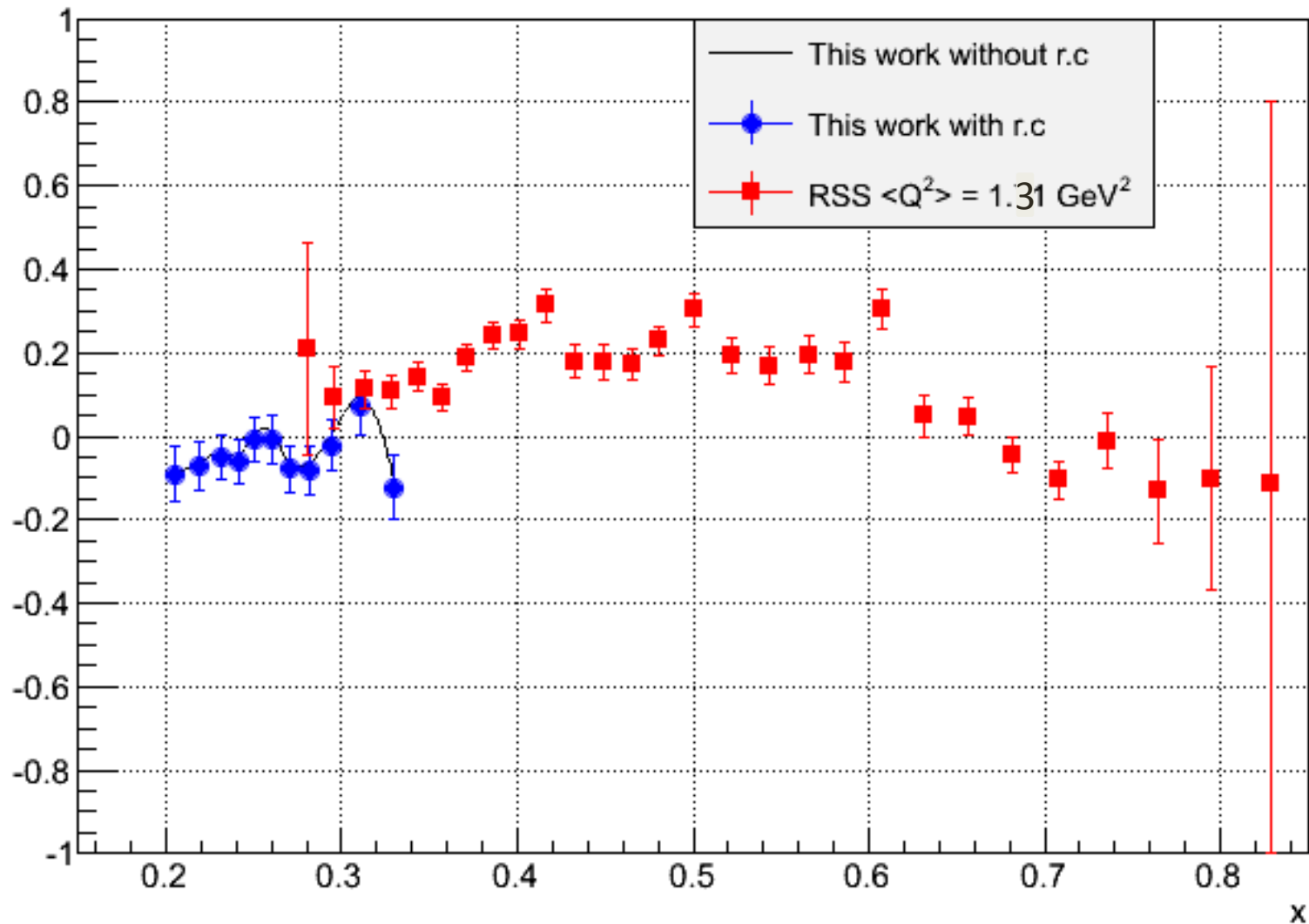
$A_2$  along  $W$



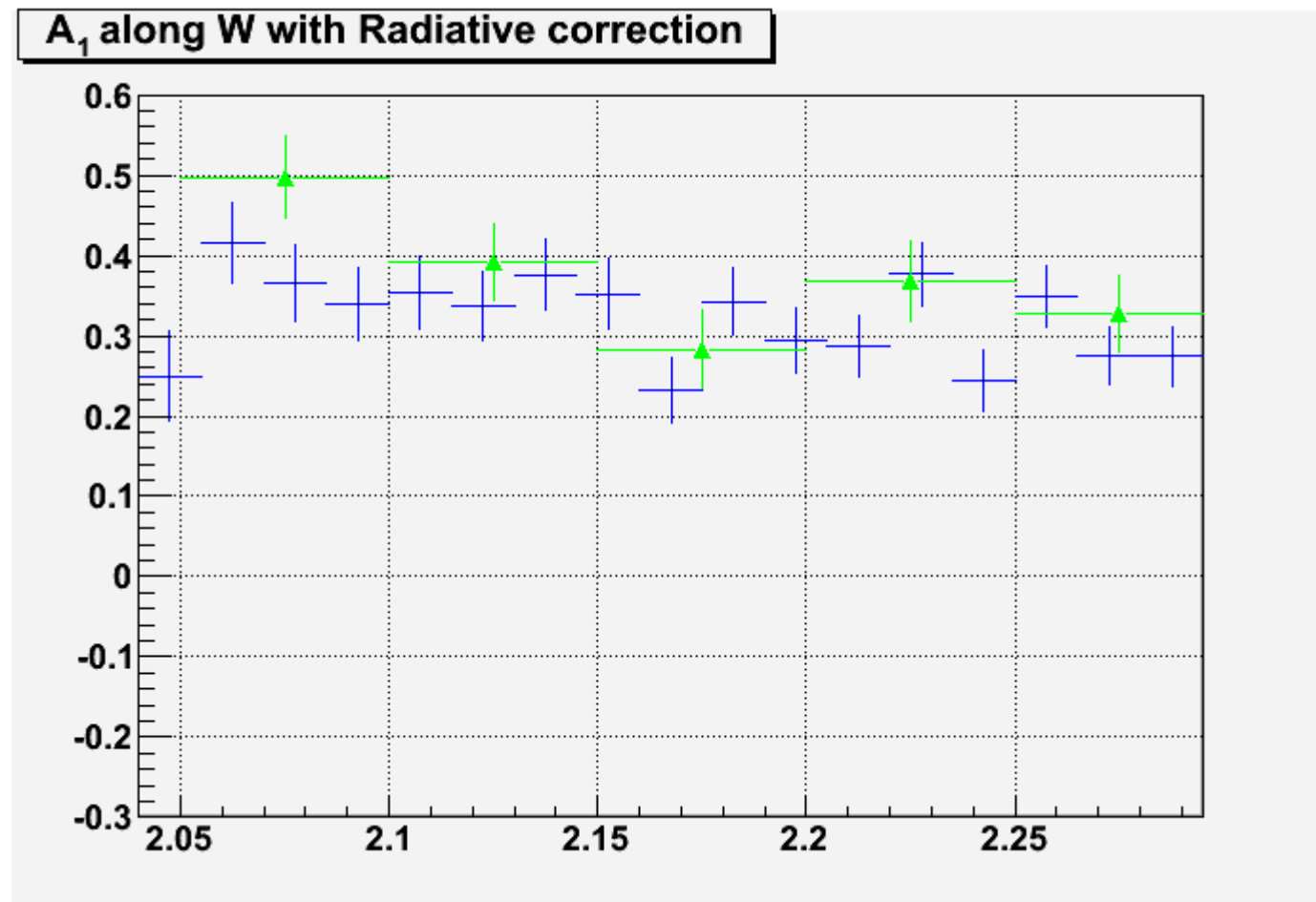


# Continuity with RSS

$A_2$  along  $x$



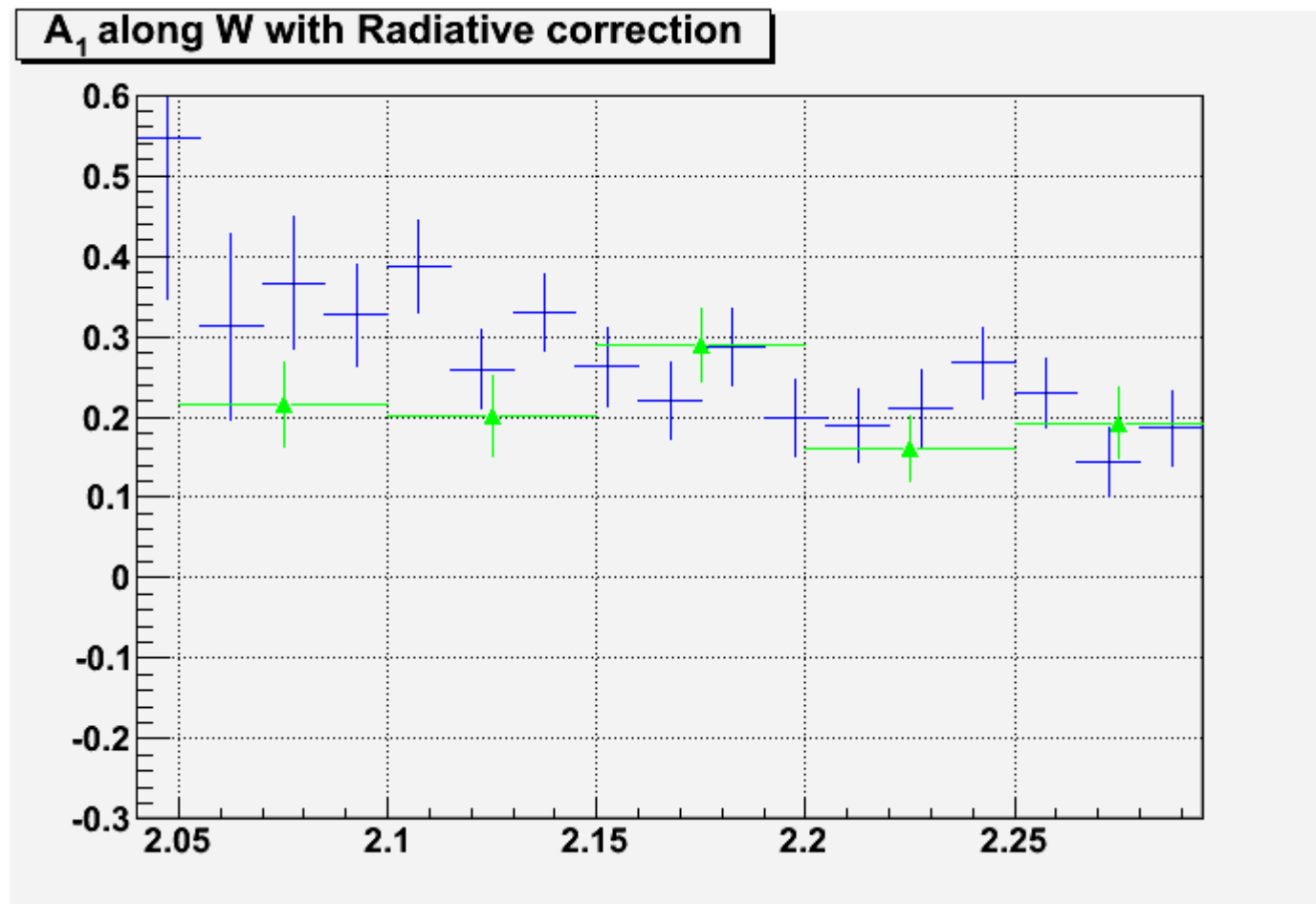
$$\text{Asymmetry } A_1 = \frac{\sigma_{TT}}{\sigma_T}$$



▲ Green triangles : CLAS EG1b result with  $Q^2 = 1.2 \text{ GeV}^2$

— Blue line : This work with  $Q^2 = 1.313 \text{ GeV}^2$

$$\text{Asymmetry } A_1 = \frac{\sigma_{TT}}{\sigma_T}$$



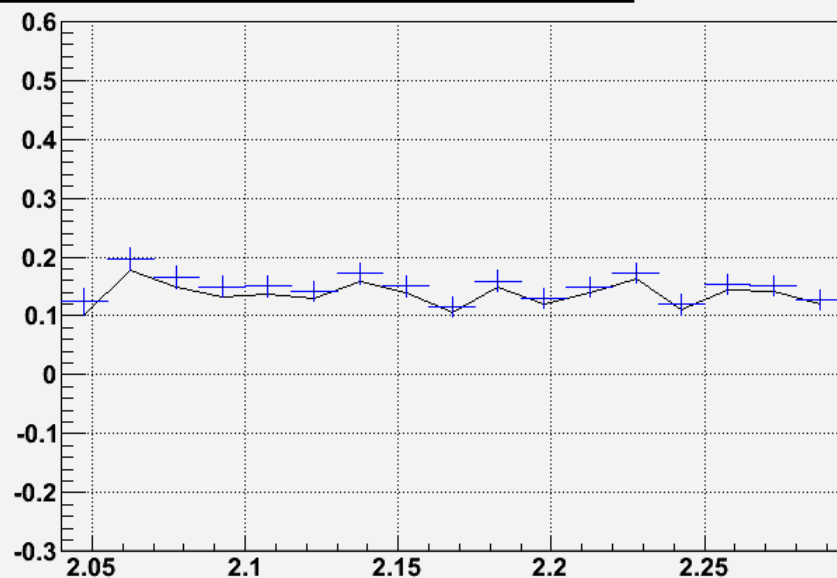
▲ Green triangles : CLAS EG1b result with  $Q^2 = 0.844 \text{ GeV}^2$

— Blue line : This work with  $Q^2 = 0.806 \text{ GeV}^2$

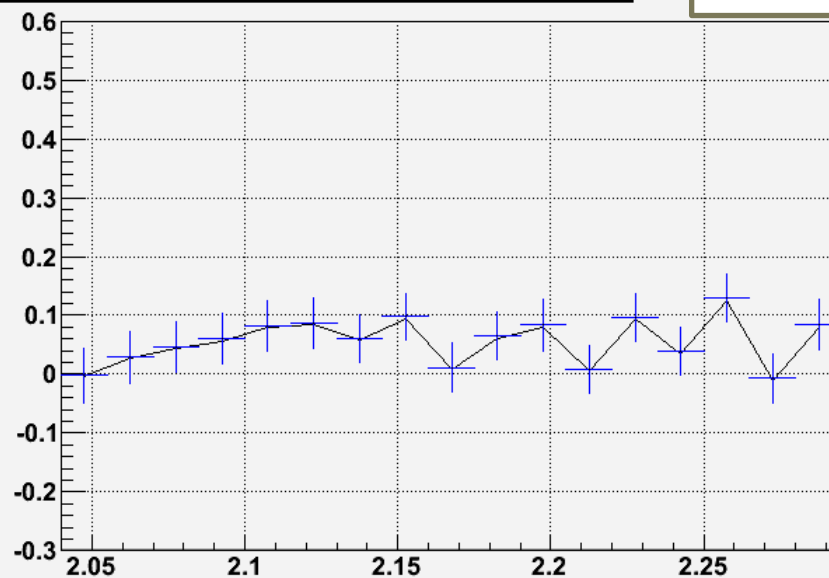
# Preliminary Asymmetries (2)

$$Q^2 = 1.313 \text{ GeV}^2$$

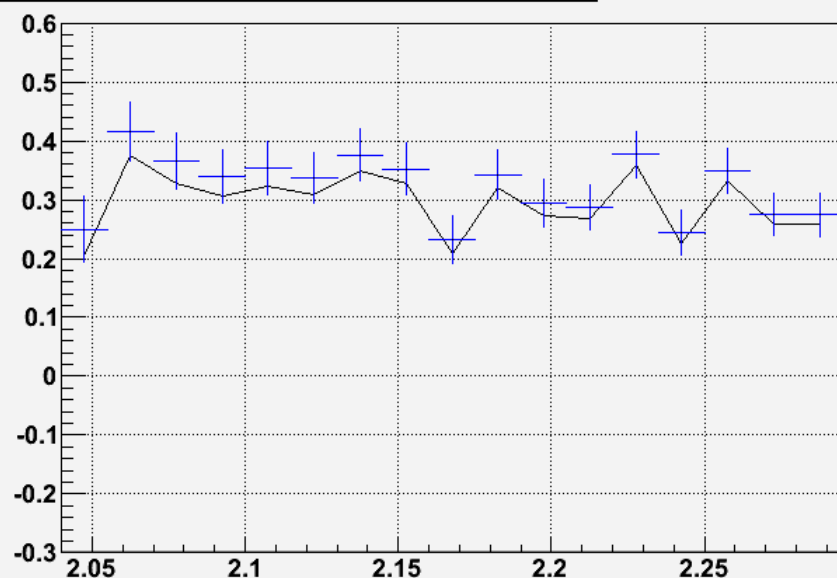
$A_{\text{para}}$  along W with(out) Radiative correction



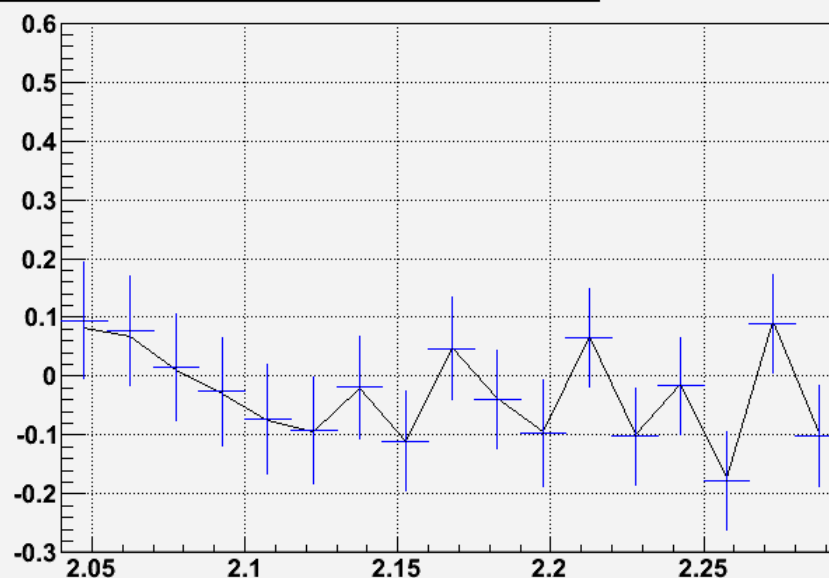
$A_{\text{perp}}$  along W with(out) Radiative correction



$A_1$  along W with(out) Radiative correction



$A_2$  along W with(out) Radiative correction

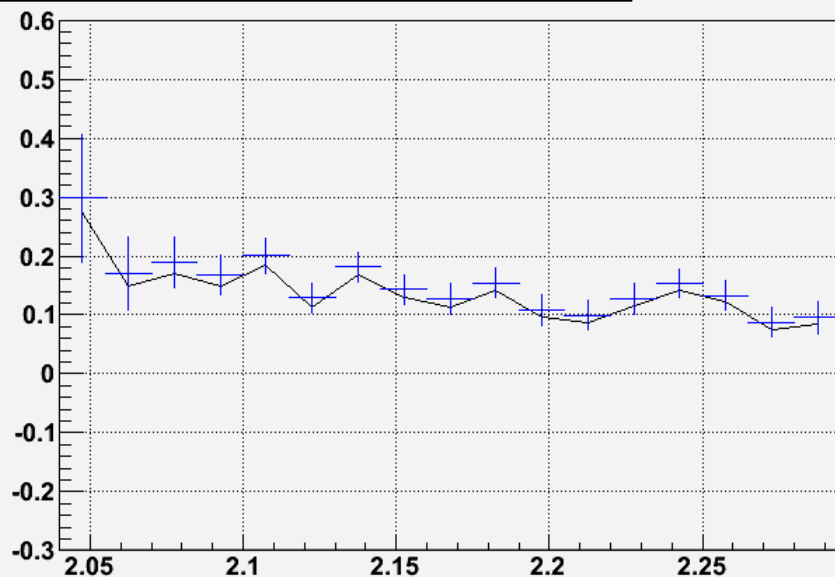


Very Preliminary

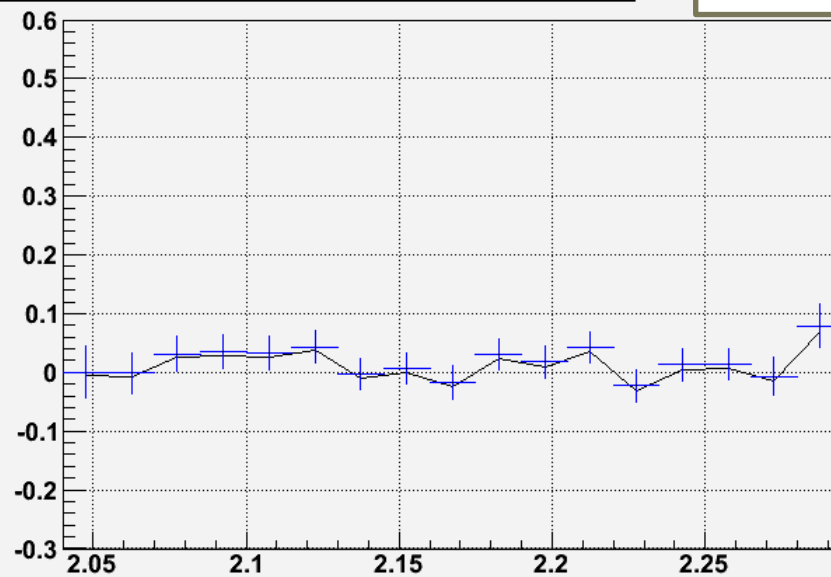
# Preliminary Asymmetries (3)

$$Q^2 = 0.806 \text{ GeV}^2$$

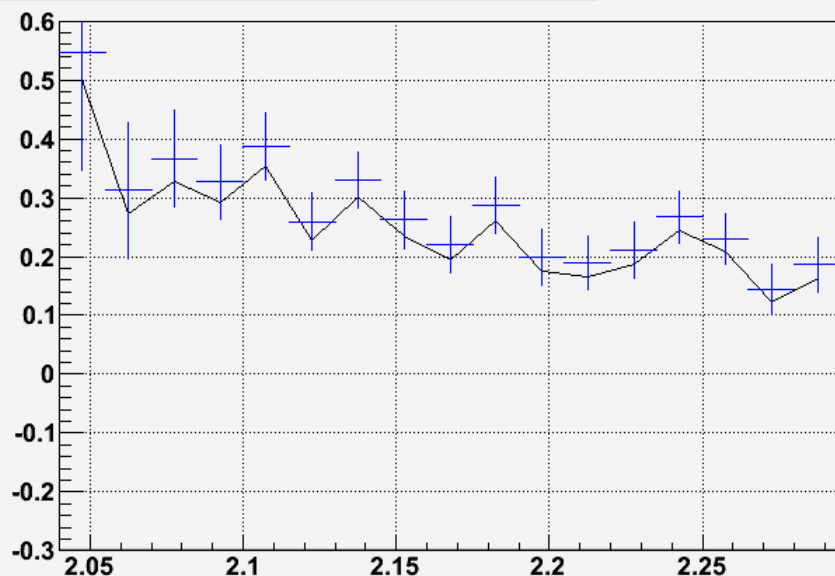
$A_{\text{para}}$  along W with(out) Radiative correction



$A_{\text{perp}}$  along W with(out) Radiative correction

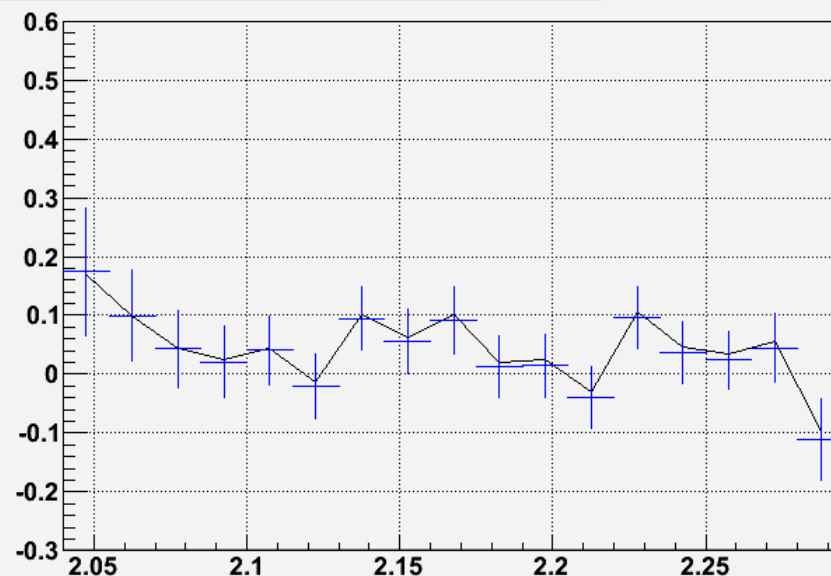


$A_1$  along W with(out) Radiative correction



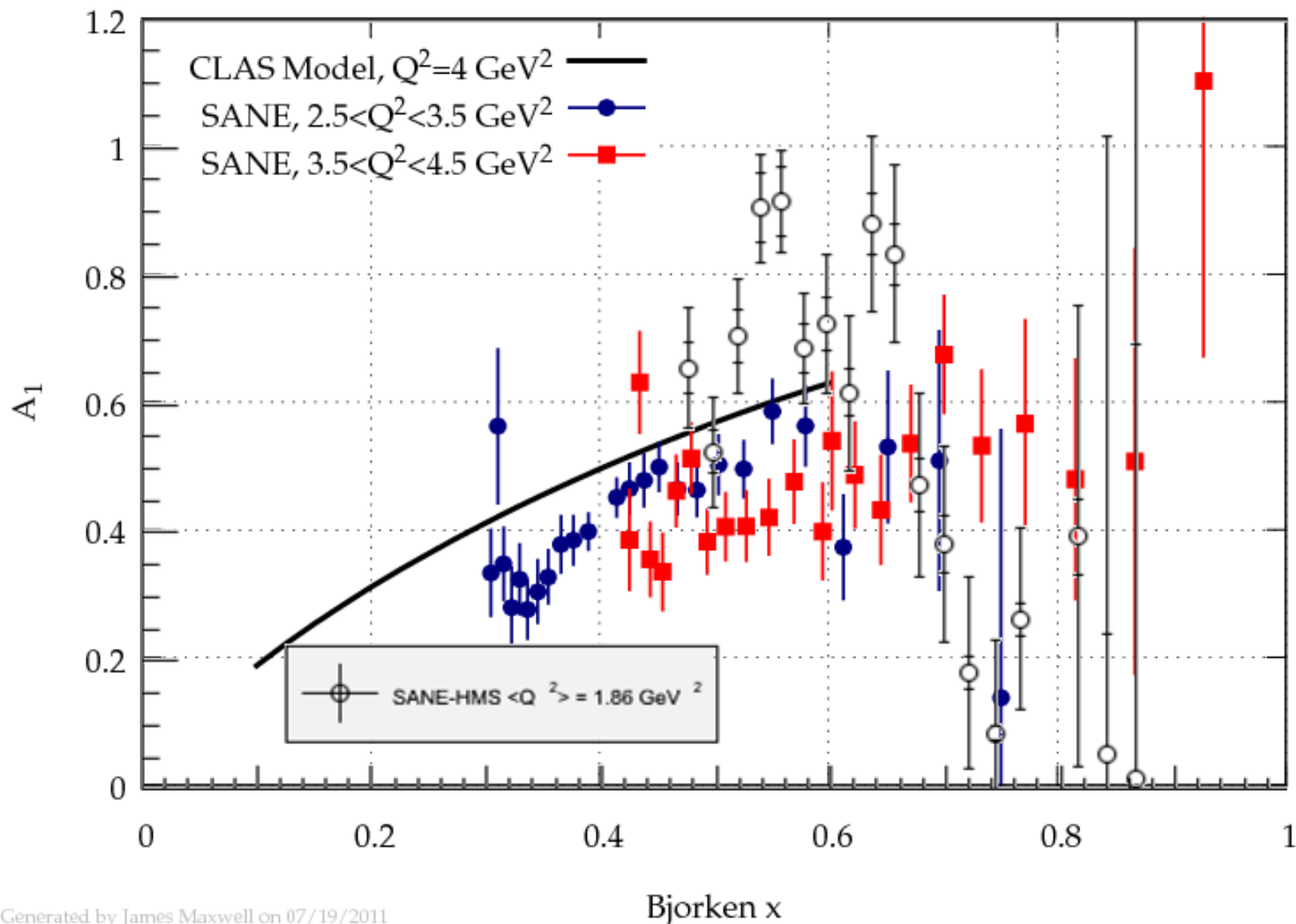
Very Preliminary

$A_2$  along W with(out) Radiative correction



# SANE-HMS and SANE-BETA

Very Preliminary  $A_1^P$ , Statistical Errors

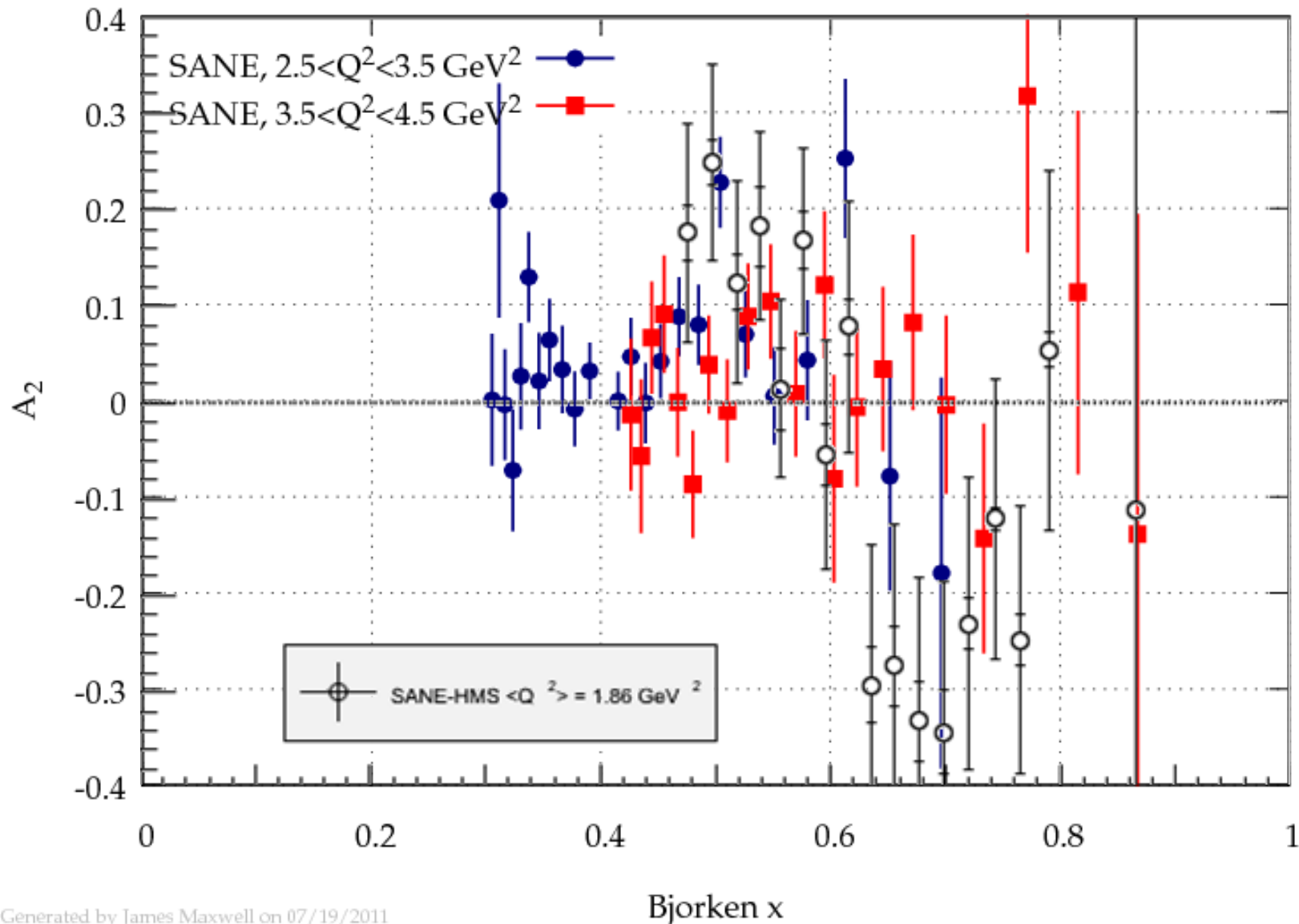


Generated by James Maxwell on 07/19/2011

BETA analyzed by J. Maxwell (UVA)

# SANE-HMS and SANE-BETA

Very Preliminary  $A_2^P$ , Statistical Errors

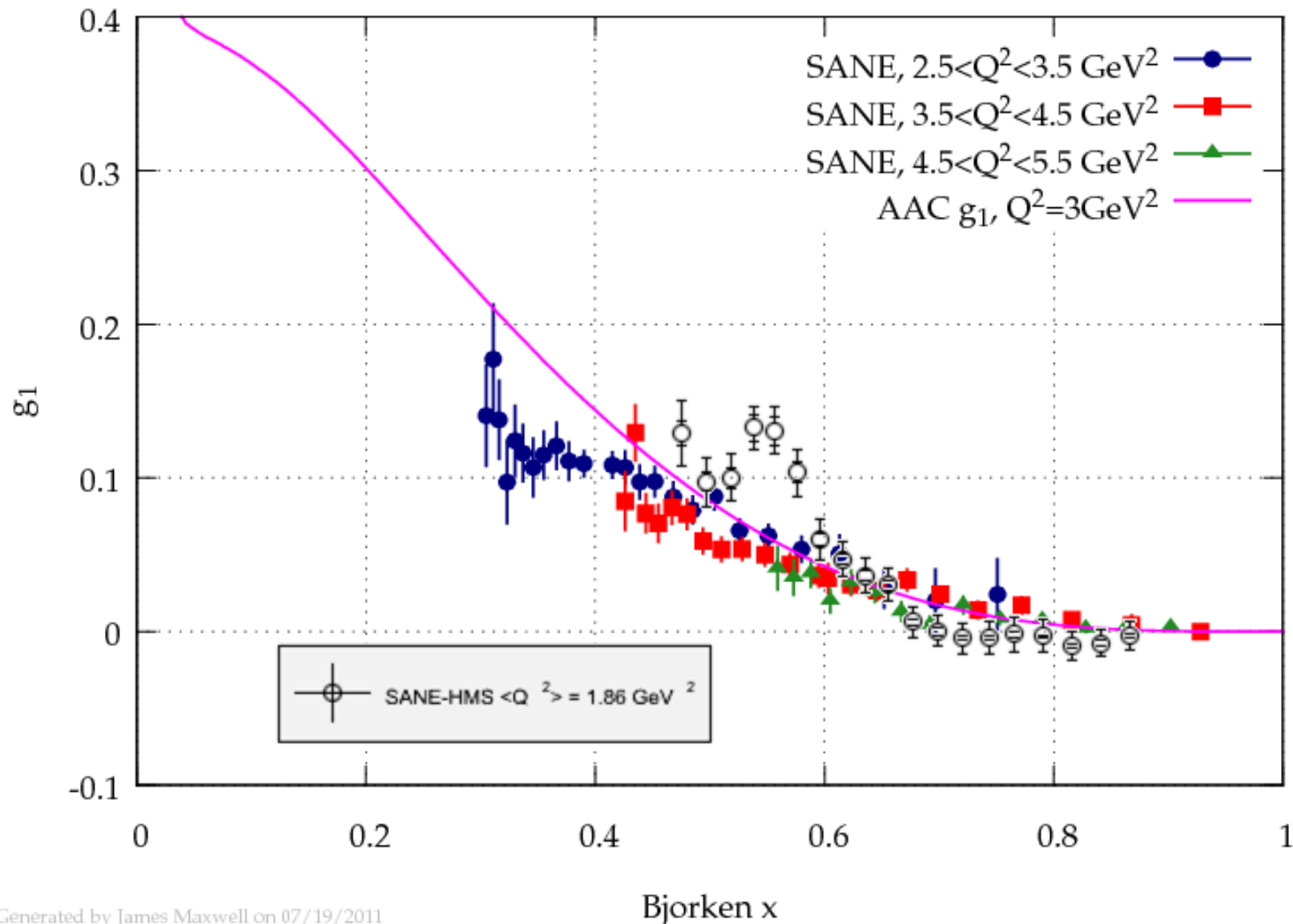


Generated by James Maxwell on 07/19/2011

BETA analyzed by J. Maxwell (UVA)

# SANE-HMS and SANE-BETA

Very Preliminary  $g_1^p$ , Statistical Errors



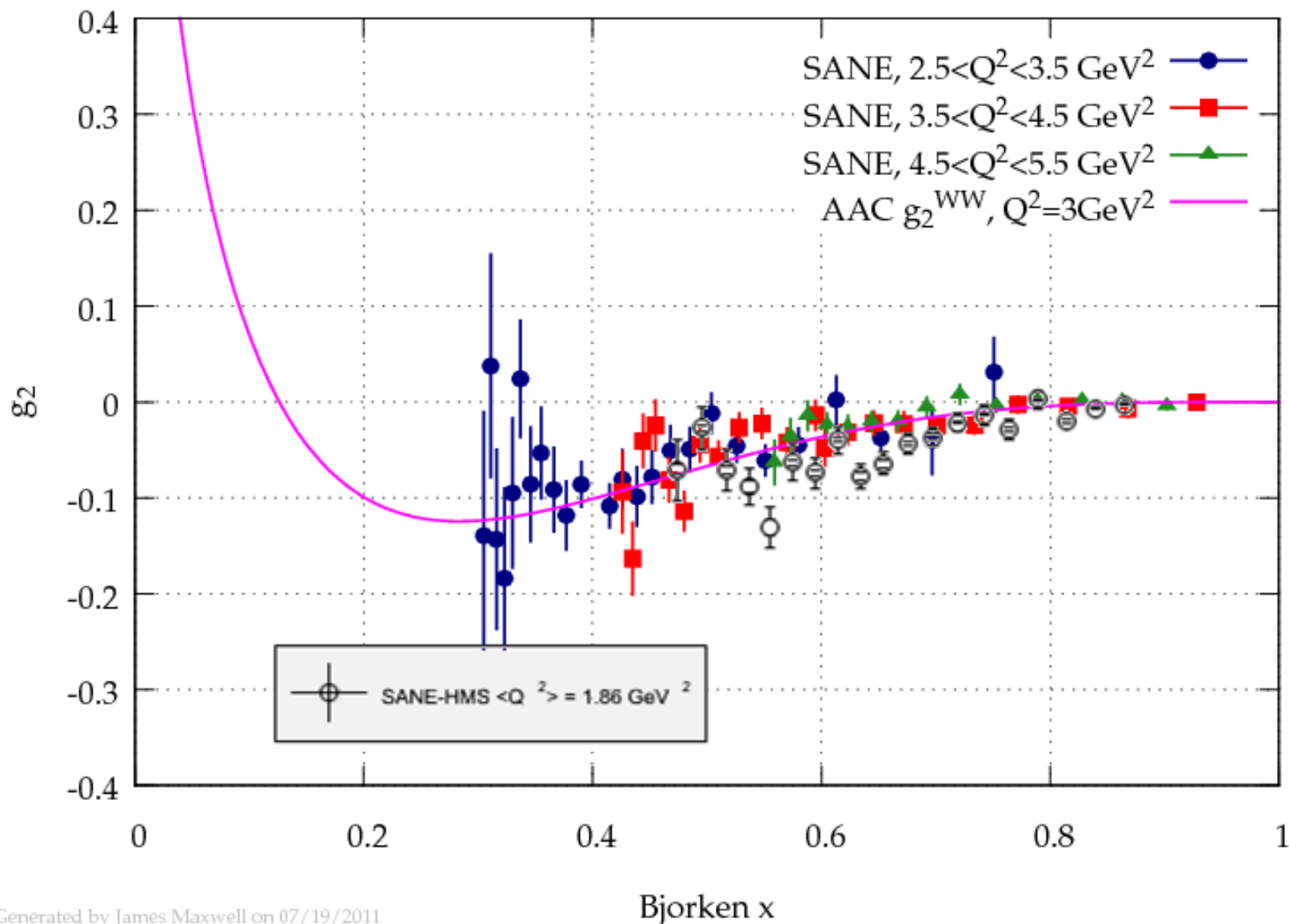
Generated by James Maxwell on 07/19/2011

BETA analyzed by J. Maxwell (UVA)



# SANE-HMS and SANE-BETA

Very Preliminary  $g_2^p$ , Statistical Errors



Generated by James Maxwell on 07/19/2011

BETA analyzed by J. Maxwell (UVA)

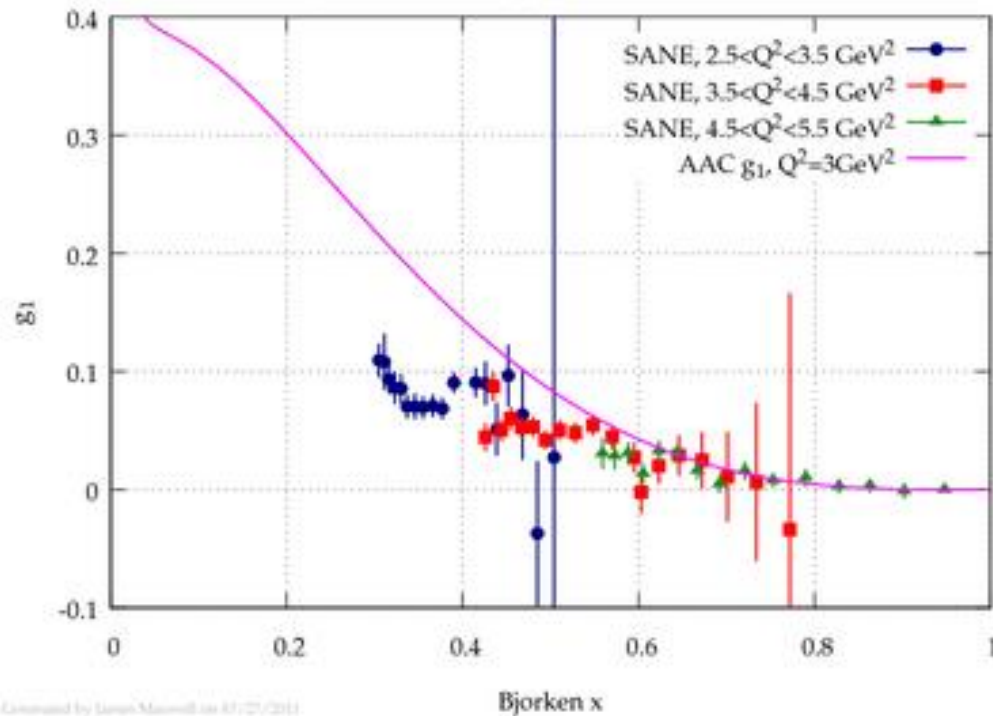
# Systematic Errors

Error Source	Average
Target Polarization	4.0%
Beam polarization	1.5%
Dilution Factor	3.0%
Radiative Corrections	10.4%
Kinematic Reconstruction	0.4%

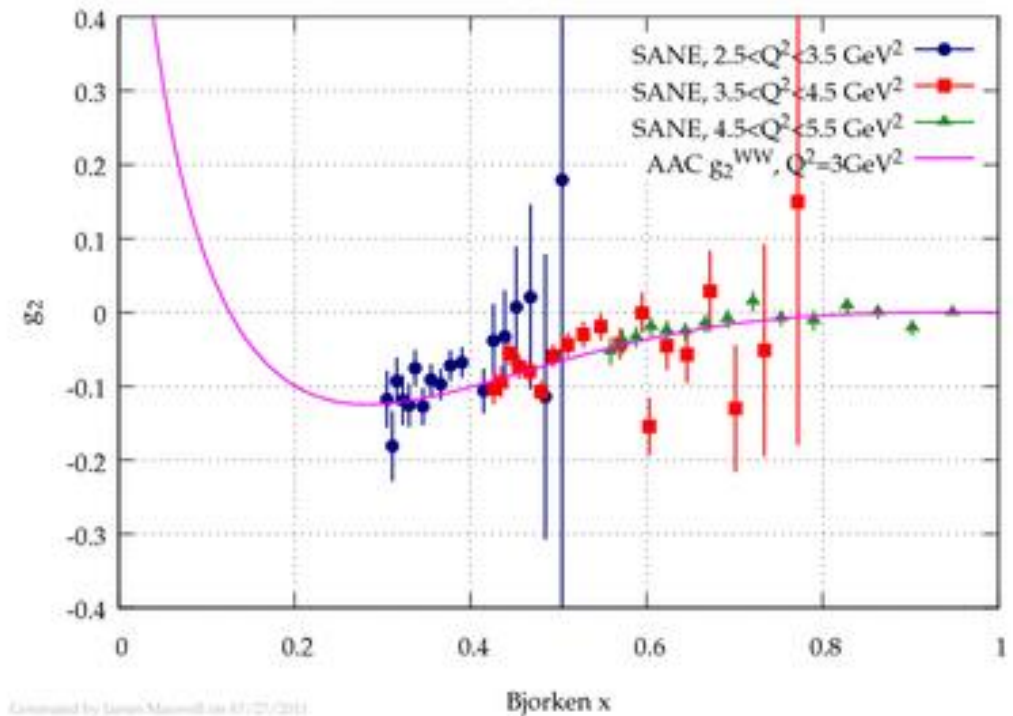
---

# Preliminary $g_1$ and $g_2$ from BETA

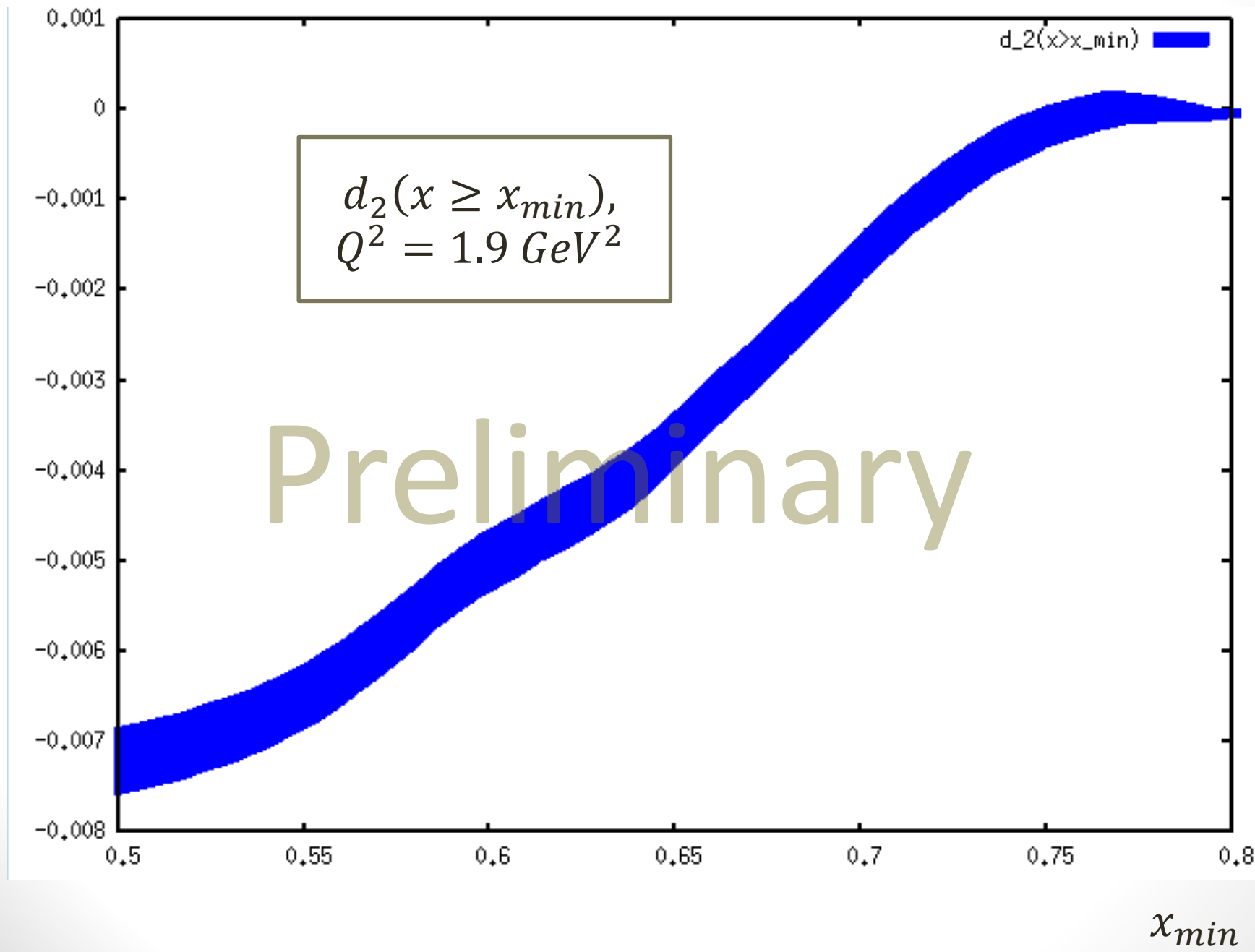
Very Preliminary  $g_1^P$ , Statistical Errors



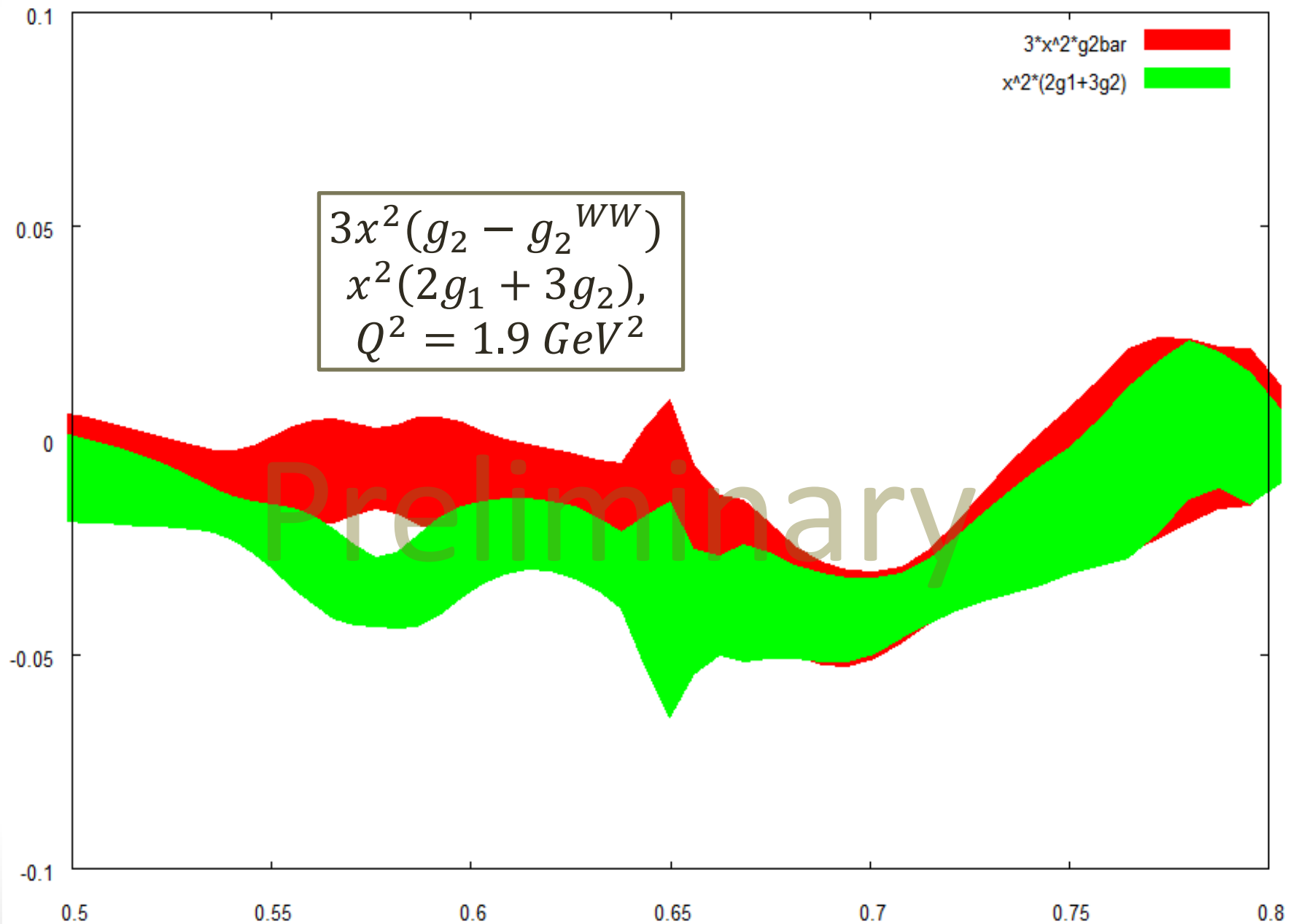
Very Preliminary  $g_2^P$ , Statistical Errors



# Twist-3 matrix element $d_2$

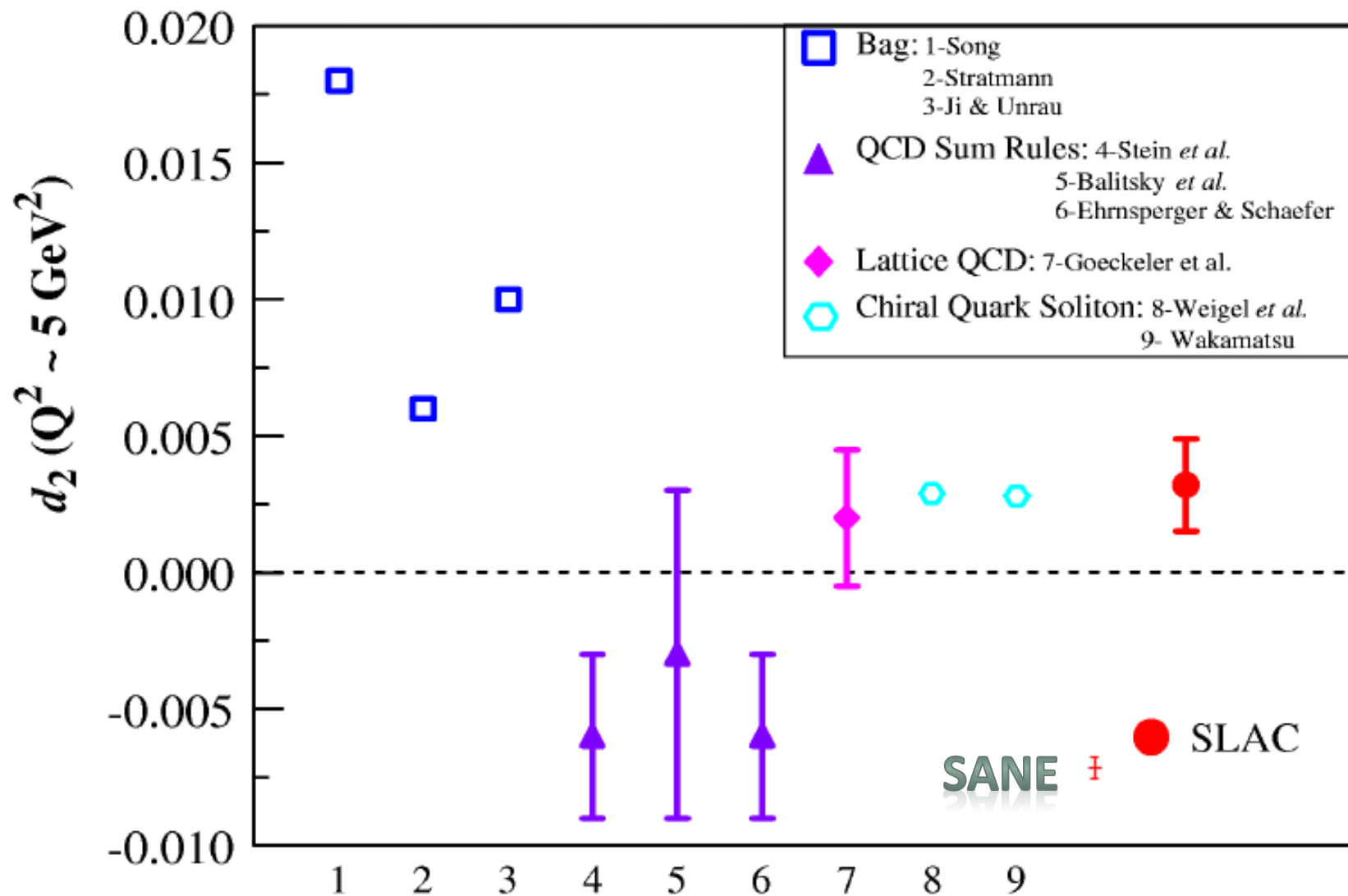


# Twist-3 matrix element $d_2$



$x$

# Twist-3 matrix element $d_2$



# RSS Experiment Results

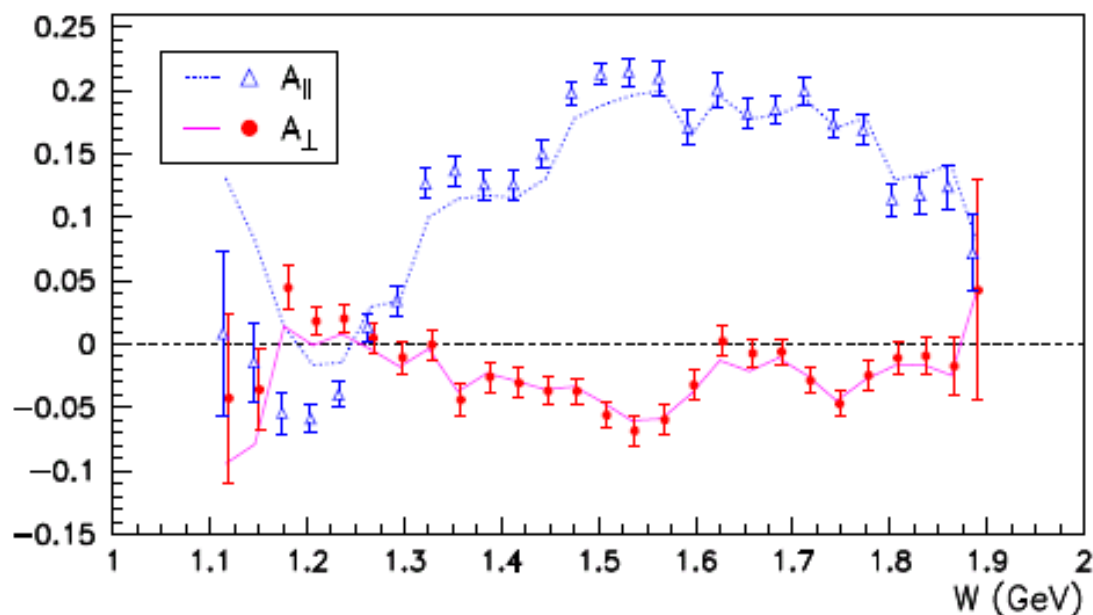


FIG. 1: Our measured asymmetries  $A_{\parallel}$  and  $A_{\perp}$ , fully corrected (points) and without radiative corrections (curves).

TABLE I: Averaged systematic errors in the asymmetries.

Error Source	$A_{\parallel}$	$A_{\perp}$
Target Polarization	} 1.1 %	2.9 %
Beam Polarization		1.3 %
Dilution Factor	4.9 %	4.9 %
Radiative Corrections	2.7 %	12.9 %
Kinematic Reconstruction	0.4 %	0.4 %

Phys. Rev. Lett. 98, 132003 (2007)

# RSS Experiment Results

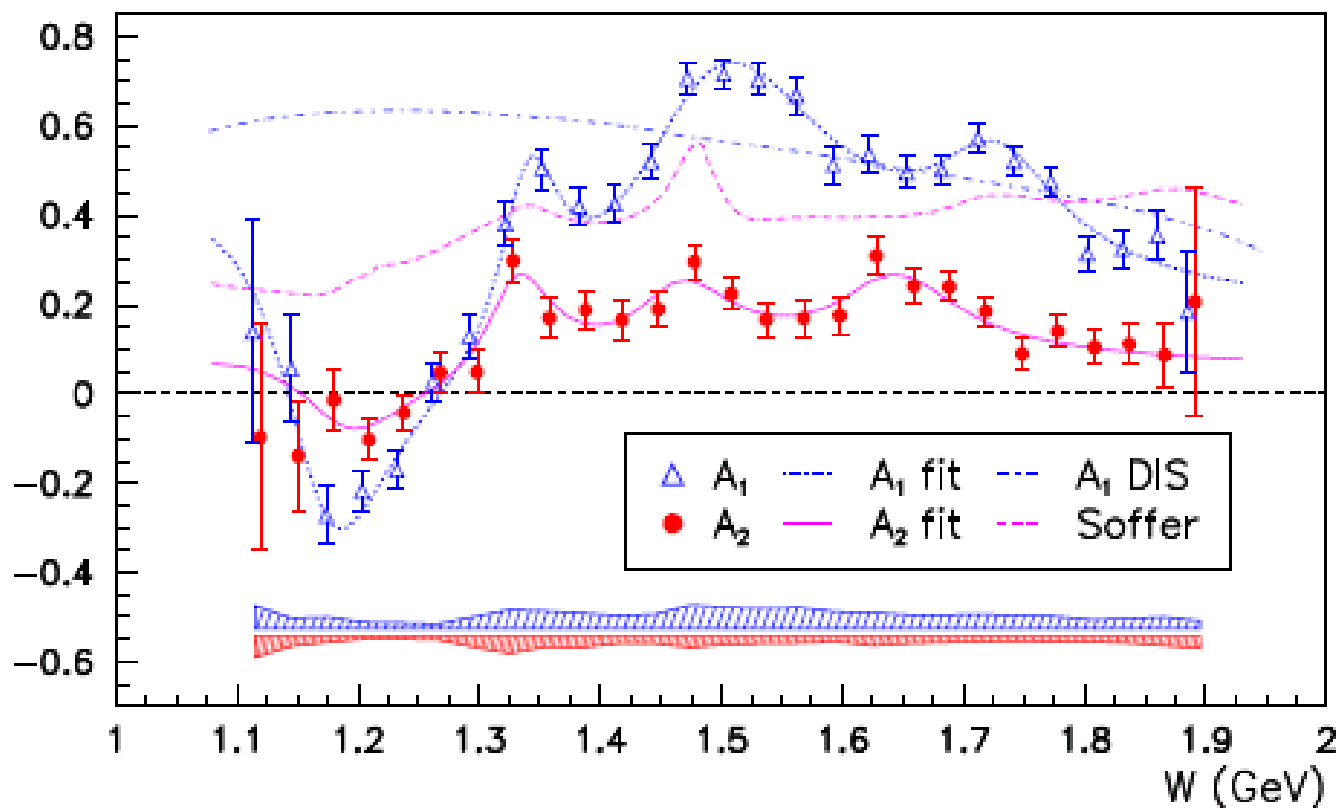


FIG. 2: Virtual photon asymmetries  $A_1$  and  $A_2$  from our data and corresponding fits. Also shown is the E155 fit to DIS data [25, 26], evaluated at our  $(x, Q^2)$ , and the Soffer limit for  $A_2$  [31], based on our  $A_1$  fit. The upper error band indicates the systematic error in  $A_1$ , the lower one  $A_2$ .



# RSS Experiment Results

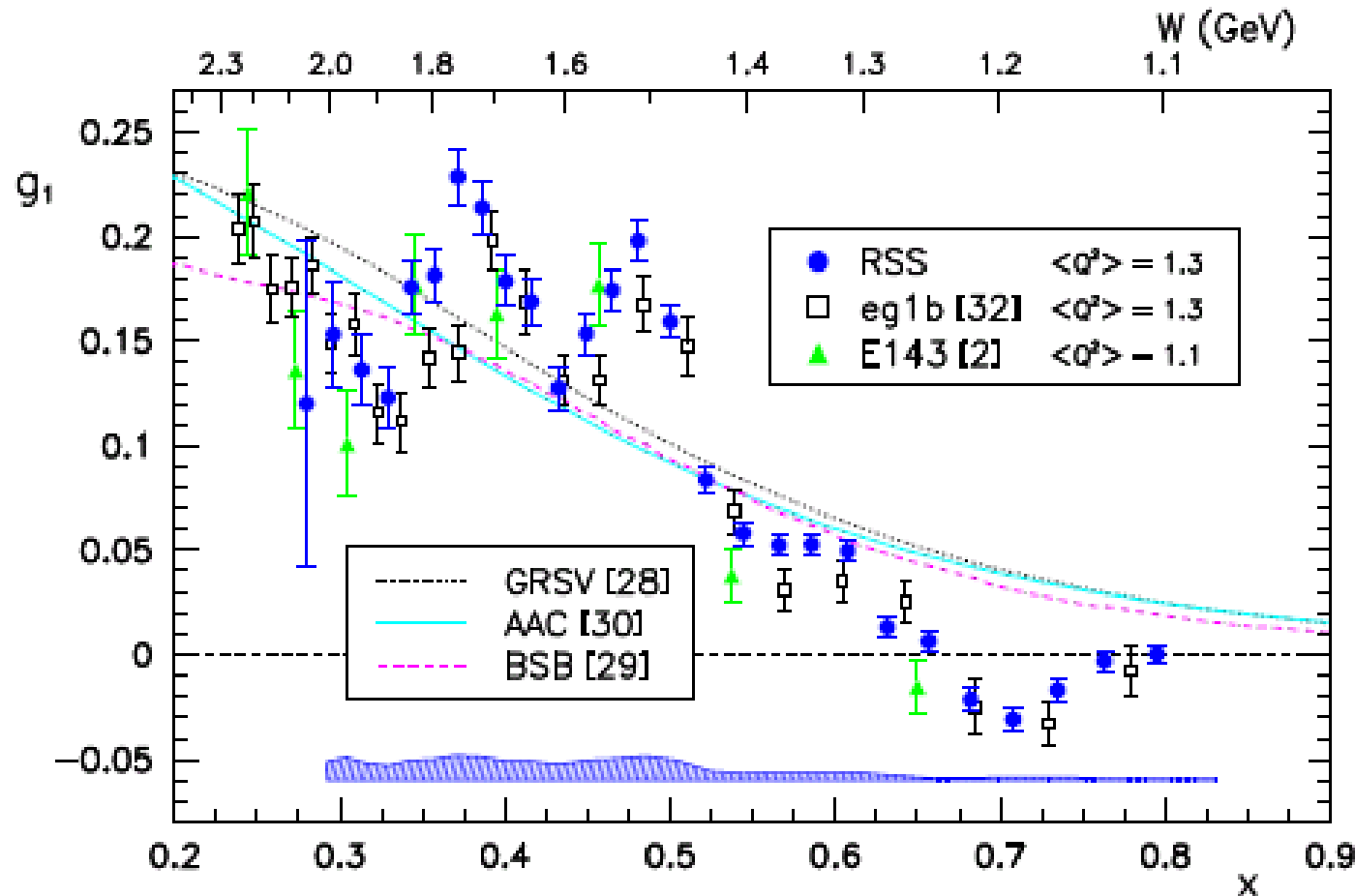


FIG. 3: Results for  $g_1$  from this experiment (RSS) and other relevant data [2, 32], as well as target mass corrected NLO PDFs. The upper scale shows  $W$  (at  $Q^2 = 1.3 \text{ GeV}^2$ ) for reference.

Phys. Rev. Lett. 98, 132003 (2007)

# RSS Experiment Results

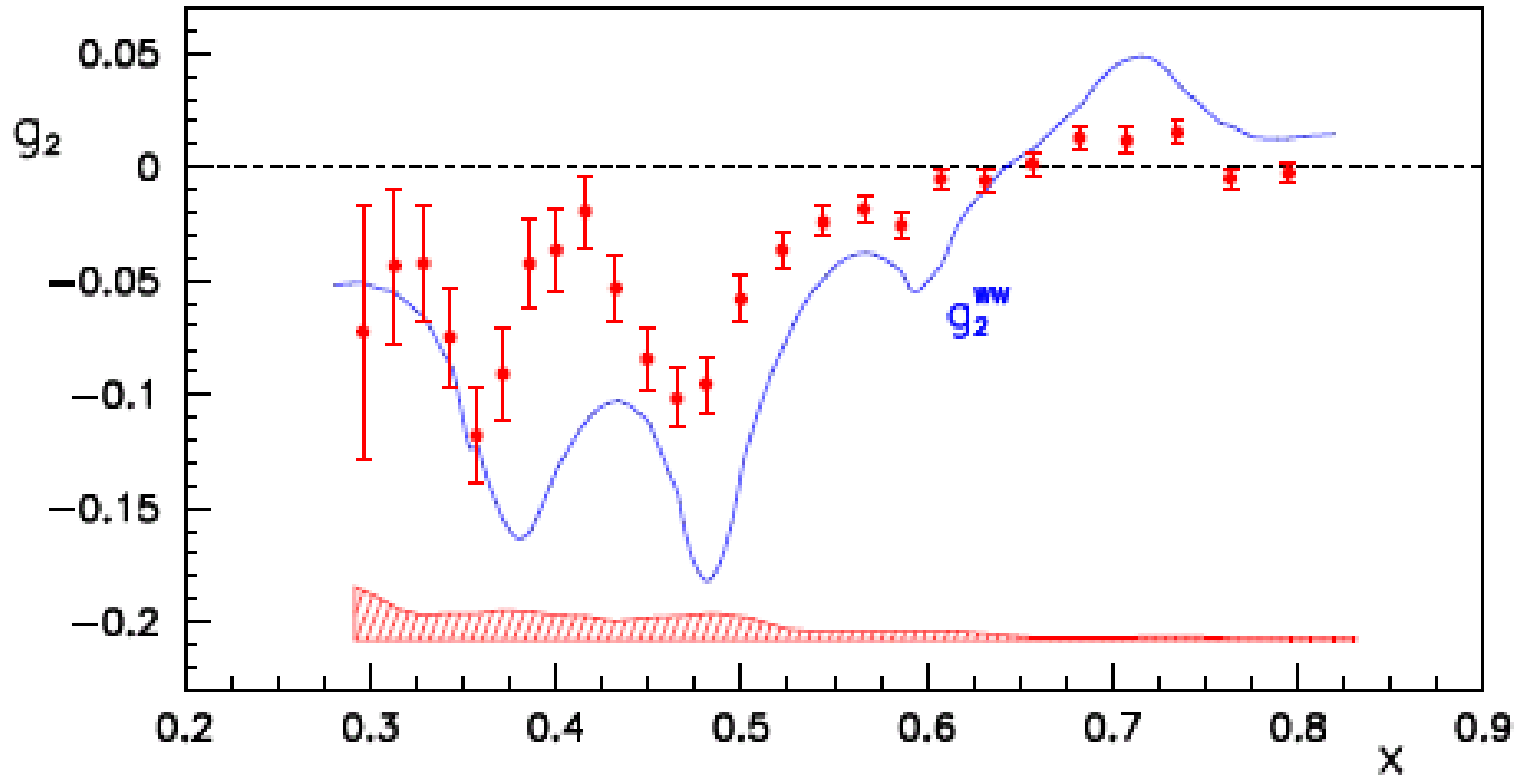
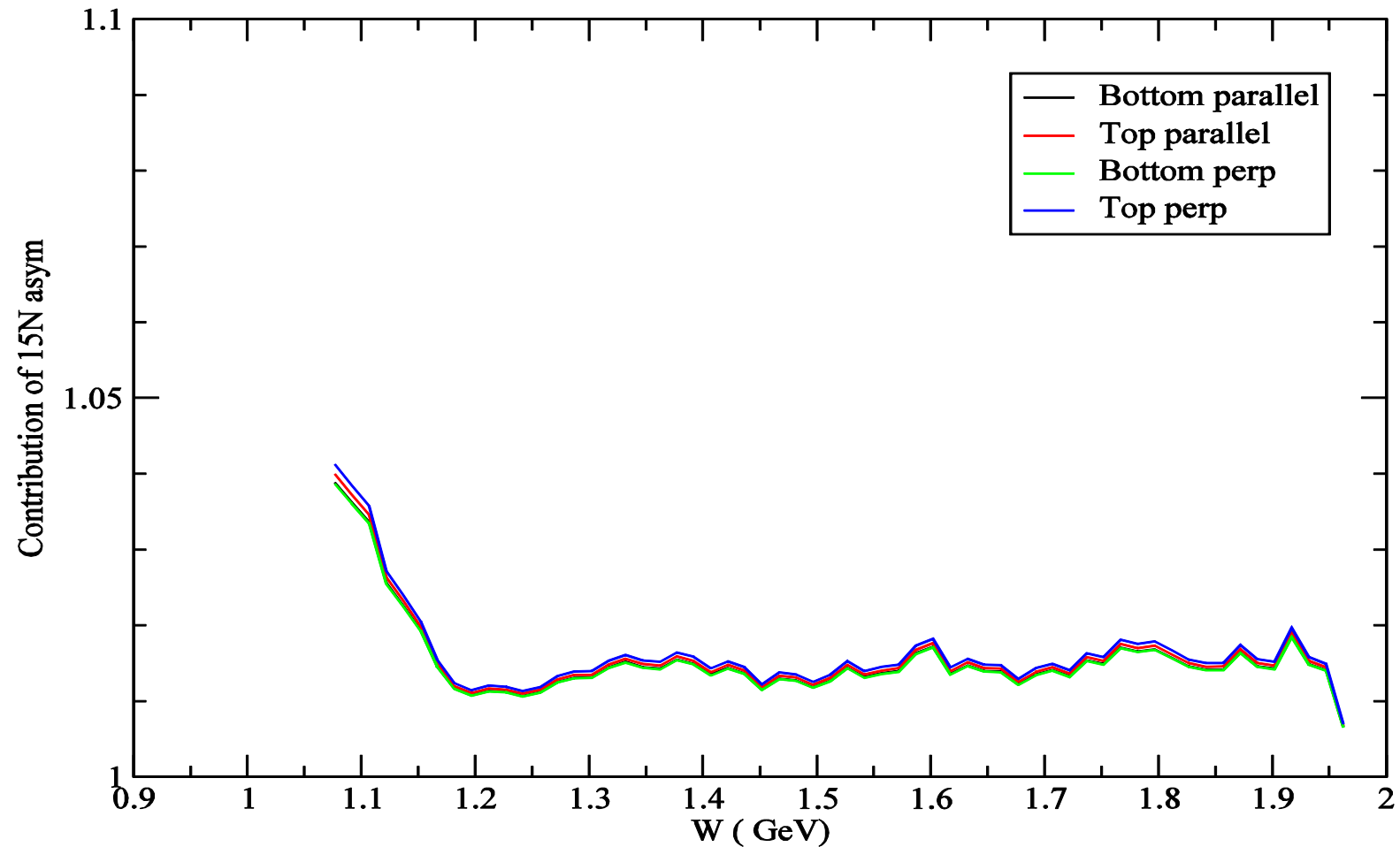


FIG. 4: Our (RSS) values for  $g_2$  and the approximation  $g_2^{ww}$  (Eq. 1) as evaluated from our data.

# Nitrogen Correction

Contribution of 15N asym



# Borrowed Slides

## Transverse Spin Structure Function

- Polarized longitudinal structure function has simple parton model interpretation

$$g_1(x) = \sum e_i^2 \Delta q_i(x), \quad i = u, \bar{u}, d, \bar{d} \dots$$

- $g_2$  is combination of twist-2 and twist-3 components:

$$\begin{aligned} g_2(x, Q^2) &= g_2^{WW}(x, Q^2) + \bar{g}_2(x, Q^2) \\ &= -g_1(x, Q^2) + \int_x^1 g_1(x', Q^2) \frac{dx'}{x'} - \int_x^1 \frac{\partial}{\partial x'} \left[ \frac{m}{M} h_T(x', Q^2) + \xi(x', Q^2) \right] \frac{dx'}{x'} \end{aligned}$$

- Wandzura-Wilczek  $g_2^{WW}$  depends on  $g_1$ ;  $h_T$  is twist-2 chiral odd transversity
- $\xi$  represents quark-gluon correlations (twist-3).
- Transverse spin structure function  $g_T$  measures spin distribution normal to virtual  $\gamma$

$$g_T = g_1 + g_2 = \int_x^1 \left[ g_1 - \frac{\partial}{\partial x'} \left( \frac{m}{M} h_T + \xi \right) \right] \frac{dx'}{x'} = \frac{\nu}{\sqrt{Q^2}} F_1(x, Q^2) A_2(x, Q^2)$$

# Borrowed Slides

## Transverse Spin Structure Sum Rules

- OPE: moments of  $g_1$ ,  $g_2$  related to twist-2 ( $a_N$ ), twist-3 ( $d_N$ ) matrix elements.

$$\int_0^1 x^N g_1(x, Q^2) dx = \frac{1}{2} a_N + O(M^2/Q^2), \quad N=0, 2, 4, \dots$$

$$\int_0^1 x^N g_2(x, Q^2) dx = \frac{N}{2(N+1)} (d_N - a_N) + O(M^2/Q^2), \quad N=2, 4, \dots$$

- $d_N$  measure twist-3 contributions (related to for  $m \ll M$  and  $h_T$  not too large.)

$$d_N(Q^2) = \frac{2(N+1)}{N} \int_0^1 x^N \overline{g}_2(x, Q^2) dx$$

- Burkhardt-Cottingham
  - not from OPE

$$\int_0^1 g_2(x) dx = 0$$

- Efremov-Leader-Teryaev
  - valence quarks combining with  $g_{2,1}^n$  from Hall A

$$\int_0^1 x (g_1^V(x) + 2 g_2^V(x)) dx = 0$$